Chapter 5. EXCITATION OF TSUNAMIS BY EARTHQUAKES

EMILE A. OKAL

Northwestern University

Contents

1. Introduction: Earthquakes
2. Generation of a tsunami by an earthquake: The classical model
3. Tsunamis as free oscillations of the Earth: the normal mode formalism
4. Earthquake tsunamis in the near field: Scaling laws and invariants
5. Earthquake tsunamis in the far field: Directivity
6. The case of "tsunami earthquakes"
7. Conclusion

References

"Comparisons suggest that each tsunami is unique and unpredictable in some respects and predictable in others.

[Fraser et al., 1959]

1. Introduction: Earthquakes

The subject of this chapter is to describe both qualitatively and quantitatively the excitation of tsunamis by earthquake sources. Indeed, most large tsunamis, and especially those destructive in the far field, are generated by earthquakes, and thus an adequate understanding of the excitation of tsunamis by earthquake sources is critical to advances in the fields of tsunami mitigation and warning. In this context, our emphasis will be the nature of the physical process of excitation of the tsunami, and the identification of general properties of earthquake-generated tsunamis which are robust invariants with respect to variations in the details of the seismic source.

1.1. The earthquake process

An earthquake consists of the release of stresses constantly accumulated under the tectonic forces applied within the Earth, when they become greater than the strength of the relevant rocks. To be considered an earthquake, this process must

The Sea, Volume 15, edited by Eddie N. Bernard and Allan R. Robinson
ISBN 978–0–674–03173–9

occur in the brittle regime, in which the failing material rebounds to its undeformed state, thereby releasing the elastic energy accumulated during the interseismic deformation, in the form of seismic waves. The failure takes place through the development of a cut of finite dimensions, or *dislocation,* in an otherwise elastic medium (the country rock). It is along this usually planar structure that the seismic slip takes place (Fig. 5-01).

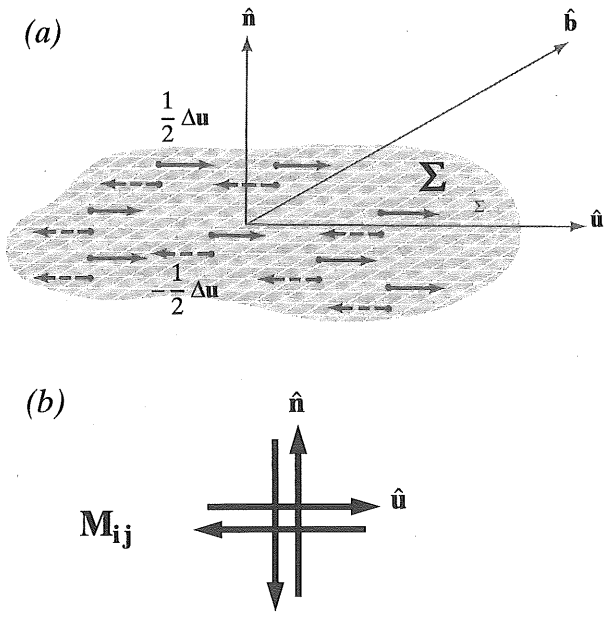

Fig. 5.01 – *(a)* Seismic slip along a fault (represented as the hatched area). The total slip Δu is the difference between the displacements of the top wall (shown as solid arrows) and of the bottom wall (dashed arrows). This dislocation, of area Σ, cut into an elastic medium, is equivalent to the *double-couple* shown in *(b),* with components in the directions of the slip vector ($\hat{\mathbf{u}}$) and of the normal to the fault plane ($\hat{\mathbf{n}}$), acting in an unruptured medium. After *Aki and Richards* [1980].

A fundamental characteristic of the earthquake source is that the extent of the dislocation is bounded in space, which amounts to saying that even though slip takes place along the fault during the earthquake, the elastic material containing the source keeps its overall cohesion. In particular, this means that it is possible to find a continuous path through unruptured material from one side of the dislocation to the other. For example and in lay terms, following a large earthquake on the San Andreas Fault, one can always drive far enough along the fault to eventually cross it *on an uncracked road,* beyond the ending point of rupture, and return to the other side uneventfully. This is of course in contrast to a *landslide* or *slump* during which the mass set in motion is permanently and totally detached from its foot wall, with no possible connection between the two sides through unperturbed material. This apparently trivial remark is at the core of the physical differences between earthquake and landslide sources, and has far-reaching consequences on their respective properties, including their potential for tsunami generation.

Because the earthquake fault is finite, and the elastic material extends continuously beyond the end of the fault, the seismic slip Δu is limited by the length L of

the fault. Within a geometrical factor of order one, their ratio is governed by the maximum strain allowed by the strength of the rock, ε_{max}. For a given class of rocks, this dimensionless parameter is a fundamental invariant of the seismic source, on the order of 2×10^{-4}. As a result, the earthquake process can be described as moving considerable amounts of matter over relatively short distances: the maximum documented value of seismic slip Δu is about 15 to 20 m, during gigantic earthquakes such as Chile (1960) or Sumatra (2004), even though these events had fault ruptures extending 800 and 1200 km, respectively [*Plafker and Savage,* 1970; *Banerjee et al.,* 2007]. Furthermore, because the walls of the fault move a relatively short distance Δu during a seismic event, the duration of this motion, called *rise time* τ, is always very short, usually a few seconds, and at most a few tens of seconds for the largest events. The total source duration of an earthquake is then controlled by the *propagation* of the rupture along the potentially very long fault zone, which can last at most $t_R = 10$ mn for gigantic events such as Sumatra (2004).

This is in contrast to landslides, which displace relatively small amounts of material (rarely exceeding 10 km in size), over distances comparable to, or greater than, their own dimensions, and which can last as much as several hours if they develop into underwater turbidity currents [*Schwarz,* 1982].

1.2. Representation of the earthquake source; the seismic moment M_0

During an earthquake, the Earth as a global system is deformed, but remains isolated in space, and thus receives no linear or angular momentum. This remark explains the unsuccessful attempts, prior to the 1950s, to represent the earthquake source with a single force or a couple of forces exerting a torque on the planet. Rather, the theoretical description of a seismic source uses a system of forces called a double-couple, a concept introduced originally by *Vvedenskaya* [1956], formalized by *Knopoff and Gilbert* [1959], and first applied to the quantification of an earthquake by *Aki* [1966]. In this framework, the earthquake is modeled using a second-order symmetric moment tensor $\mathbf{M}$, whose only non-zero components are those indexed along the direction of seismic slip, $\hat{\mathbf{u}}$, and the direction normal to the fault plane, $\hat{\mathbf{n}}$:

$$\mathbf{M} = M_0 \, (\hat{\mathbf{u}}\hat{\mathbf{n}} + \hat{\mathbf{n}}\hat{\mathbf{u}}) \tag{1}$$

where the scalar M_0, known as the *seismic moment* of the earthquake, takes the value

$$M_0 = \mu \, \Sigma \, \Delta u \tag{2}$$

μ being the rigidity of the source rocks, Σ the area of faulting, and Δu the amplitude of the seismic slip[1]. The representation theorem forming the basis of quantita-

[1] Here, the notation, $\mathbf{a}\,\mathbf{b}$ means the column vector $\mathbf{a}$ multiplied on its *right* by the row vector $\mathbf{b}^T$, which is the transposed of the column vector $\mathbf{b}$. The result is thus a 3×3 tensor, as opposed to the case of a *left* multiplication, which would yield the 1×1 classic scalar product $\mathbf{b}^T\mathbf{a} = \mathbf{b} \cdot \mathbf{a}$.

tive seismology then states that the response of the Earth to the slip on the bounded dislocation cut into the elastic medium (as shown in Fig. 5-01*a*) is equivalent to that of the unfractured medium to the system of forces represented by (1) and shown on Fig. 5-01*b*. The latter can be used as a forcing term in the equations of dynamics to model the excitation and the propagation of all seismic waves, including, as we shall see, tsunamis.

The derivation of the representation theorem is given in all advanced seismology textbooks [*e.g., Aki and Richards,* 1980], and will not be repeated. It is important however to note that it involves integration by parts, using the familiar argument of a surface of integration sufficiently distant from the source that the fully integrated term vanishes. As noted by *Dahlen* [1993], this requires that the unperturbed medium be continuous around the source, and thus cannot be applied to the case of a landslide or slump, in which it leads to additional source terms in the representation theorem. The latter express mathematically the fundamental difference in material properties between the two kinds of sources.

It can be verified from (1) that the description of a seismic moment tensor $\mathbf{M}$ requires 4 real numbers. The latter can be expressed as the three components of the seismic slip vector $[\mu \Sigma \Delta \mathbf{u}]$, plus the orientation in space of the fault normal $\hat{\mathbf{n}}$, or alternatively, the scalar moment M_0 and three angles orienting the process in space. The latter representation emphasizes the common physical nature of earthquake sources, individual events differing only through an Euler solid rotation of the source, with the three familiar angles (strike ϕ and dip δ of fault, and rake λ of the slip on the fault plane) merely describing the orientation of the process with respect to a practical system of coordinates (vertical, North, East) at the epicenter. This remark explains that the seismic moment M_0 is the primary descriptor of the "size" of an earthquake, and consequently of the excitation and generation of all waves, seismic and others, including tsunamis, whose amplitudes are only moderately affected by the other parameters, namely the three angles describing the geometry of rupture. Conversely, M_0 (and more generally the full seismic moment tensor $\mathbf{M}$) can be inverted from extensive datasets of seismic waves, a procedure pioneered in the pre-digital era by *Gilbert and Dziewonski* [1975] and now used routinely by automated algorithms operating in quasi-real time at various data centers worldwide [*e.g., Dziewonski et al.,* 1981].

The seismic moment M_0 defined by (2) is often expressed as a so-called moment magnitude, $M_w = (\log_{10} M_0 - 16.1)/1.5$, introduced by *Kanamori* [1977] to coincide with conventional magnitudes in a range of earthquake sizes where the latter have started to be affected by source finiteness, without however reaching full saturation [*Geller,* 1976].

1.3. Scaling laws

The size of an earthquake will grow with the extensive parameters Σ and Δu in (2). As discussed above, earthquake rupture occurs when the strain accumulated in the source region reaches its critical value ε_{max}, leading to an expected proportionality between Δu and the fault length L. Furthermore, it is generally observed (for ex-

ample from the study of aftershock distributions) that the aspect ratio of the fault zone remains contained, and thus Σ grows like L^2, resulting in an overall proportionality between M_0 and L^3, which is generally confirmed on observational datasets [*Kanamori and Anderson,* 1975; *Geller,* 1976; *Wells and Coppersmith,* 1994], the ratio M_0/L^3 (related within a geometrical constant to the stress drop $\Delta\sigma$ of the event) being about 50 bars. The following practical formula was proposed by *Geller* [1976]

$$M_0 = 1.45 \times 10^{20} \cdot L^3 \cdot \Delta\sigma \tag{3}$$

where M_0 is in dyn*cm, $\Delta\sigma$ in bars, and L in km. Similarly, both rise time τ and rupture time t_R are expected to scale with Δu or L, and hence as $M_0^{1/3}$. Such scaling laws further simplify the interpretation of seismic sources by implying that estimates of parameters such as slip Δu and fault length L (which do not lend themselves to an easy measurement, especially under the operational constraints of real-time tsunami warning) can be obtained from the knowledge of M_0, now generally available within one hour of the occurrence of major earthquakes worldwide.

There exist cases, however, where scaling laws will be violated, under conditions of anomalous material properties in the source region, leading to low (or conversely, high) stress drops, slow rupture velocities, or unusual fault zone geometries [*Romanowicz,* 1992; *Polet and Kanamori,* 2000]. Such earthquakes can have irregular tsunami excitation, and consequently constitute a challenge for the warning community. A particular class of them, known as "tsunami earthquakes", will be discussed in Section 6.

2. Generation of a tsunami by an earthquake: The classical model

2.1. A simple model

The framework of the generation of a tsunami by an earthquake source is presented in very simple terms on Fig. 5-02. In this model, a fraction of the ocean floor is uplifted during the seismic event, displacing a volume of seawater. If this deformation occurs sufficiently fast, and neglecting the compressibility of seawater, one predicts an immediate and identical hump on the ocean surface (Frame *(b)*). However, because the ocean is fluid, this situation is of course unstable, and the hump flows sideways *(c):* this flow constitutes the tsunami *(d).* Eventually, the entire mass of water in the hump returns to the ocean surface, expected to be unchanged in the final state of equilibrium *(e),* the cross-section S of the hump being in all cases negligible compared with the total area of the ocean basin. Thus, the energy of the tsunami, expressed in detail in the Appendix, consists of the excess of potential energy of the displaced water in the hump on Frame *(b)* over its value at equilibrium in Frame *(e).* This excess, and hence the occurrence of the tsunami, results from the transfer of the mass of water from the seabed to the hump occurring out of equilibrium, *i.e.,* as a thermodynamically irreversible process. This will be the

case only if the deformation takes place rapidly, in practice faster than it takes the hump to propagate away from the epicentral area as a tsunami wave. The critical parameter in this respect is the ratio of the velocities characteristic of the propagation of seismic rupture along the fault, V_R, and of the tsunami wave, C. The former are typically around 3.5 km/s, and even for anomalously slow earthquakes, at least 1 km/s; the latter are typically 200 m/s, and never exceed 340 m/s, even in the deepest oceanic trenches. The bottom line is that seismic rupture is always hypersonic with respect to the tsunami, which justifies the arguably naive model of Fig. 5-02*b* and its use as an initial condition in most numerical simulations. By contrast, the slow tectonic deformations accumulated during the interseismic cycle involve velocities at most in the range of a few cm/yr, leaving ample time for the ocean surface to equilibrate, and thus qualifying as reversible processes generating no energy glut and no tsunami.

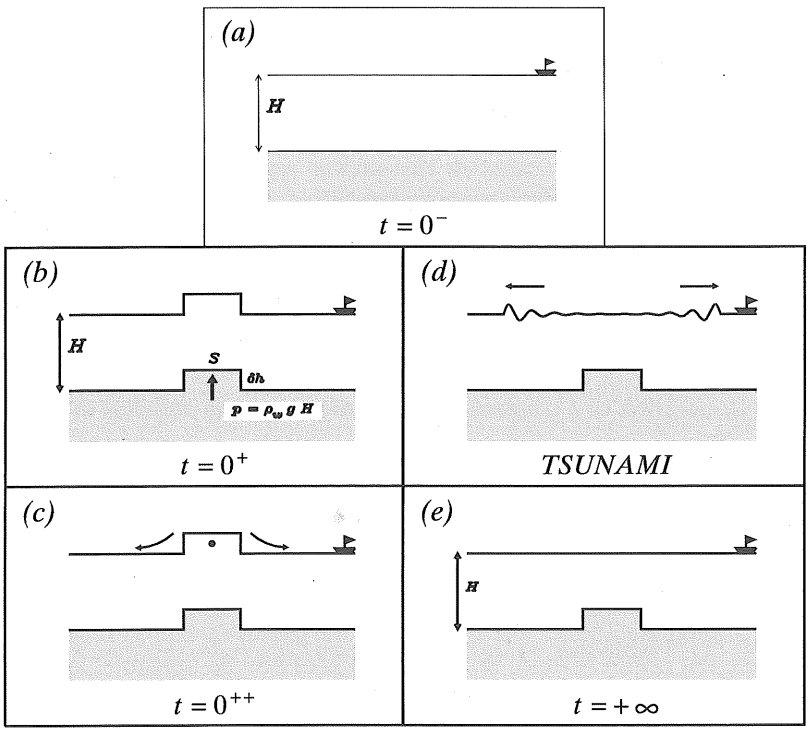

Fig. 5.02 – Sketch illustrating the excitation of a tsunami by a seismic dislocation. *(a)* Unperturbed oceanic column before the earthquake. *(b)* During the earthquake, a hump is generated on the ocean floor, resulting in an immediate and identical deformation of the ocean surface. *(c)* Because the ocean is fluid, the hump is unstable and starts flowing sideways, creating the tsunami wave *(d)*. *(e)* Eventually, at equilibrium, the ocean surface has returned to its pre-earthquake level, due to the much larger area of the ocean basin, as compared to the cross section of the hump, *S*. After *Okal* [2003].

2.2. *From earthquake seismic moment to tsunami initial conditions*

In the general framework of Fig. 5-02, it becomes possible to derive the excitation of a tsunami by computing the static field of vertical deformation u_z (x, y) of the ocean floor, and interpreting it as the field of initial displacements of the ocean surface, η (x, y).

At any point of an infinite homogeneous elastic medium, the three-dimensional static deformation incurred from a point source double-couple is obtained from the classical Somigliana tensor [*e.g., Aki and Richards,* 1980], and for an infinite half-space, there exists a formulation of the static displacement on the boundary of the medium [*Steketee,* 1958]. In the case of slip on a rectangular fault of finite size buried in a homogeneous half-space, the static solution on the surface can be worked out analytically, with independent but equivalent expressions published by *Mansinha and Smylie* [1971] and *Okada* [1985].

Such computations require the knowledge of the geometry of rupture, and of the fault parameters L, W , and Δu. For deferred simulations of the tsunamis of well-studied events, these are often available from investigations in source tomography [*e.g., Ishii et al.,* 2005] or from the combined use of the spatial extent of aftershocks and of the scalar moment M_0. In real time, under operational conditions, scaling laws such as (3) can be used to obtain estimates of L, W and Δu from an inverted value of M_0, and an estimated focal geometry can be derived from our understanding of regional plate tectonics.

As an example, Fig. 5-03 illustrates the computation of the vertical component of the static displacement, u_z , in the scenario of a repeat of the great 1833 earthquake in Southern Sumatra [*Synolakis and Okal,* 2006], based on parameters obtained from the modeling of emerged coral structures by *Zachariasen et al.* [1999]. A numerical simulation can then be launched by using the field $u_z(x, y)$ as the initial condition for $\eta(x, y)$ at time $t = 0^+$, for all points not located on initially dry land. This is complemented by setting to zero the initial field of the depth-averaged horizontal velocities of the fluid: $v_x(x, y) = v_y(x, y) = 0$. Fig. 5-04 presents the results of the simulation, using the MOST finite difference code, introduced by *Titov and Synolakis* [1998], which solves the non-linear equations of hydrodynamics in the shallow-water approximation using the method of splitting integration steps. The final product is a map of the maximum amplitude η expected during a possible repeat of the 1833 event. We stress that it is valid only on the high seas, and does not include the localized effects of shoaling and run-up at the beaches. Note the strong directivity of the wave in the far field, at right angles from the coast of Sumatra, discussed more in detail in Section 5, as well as the effect of shallow bathymetric features acting as optical lenses to focus the energy of the tsunami in the far field [*Woods and Okal,* 1987; *Satake,* 1988].

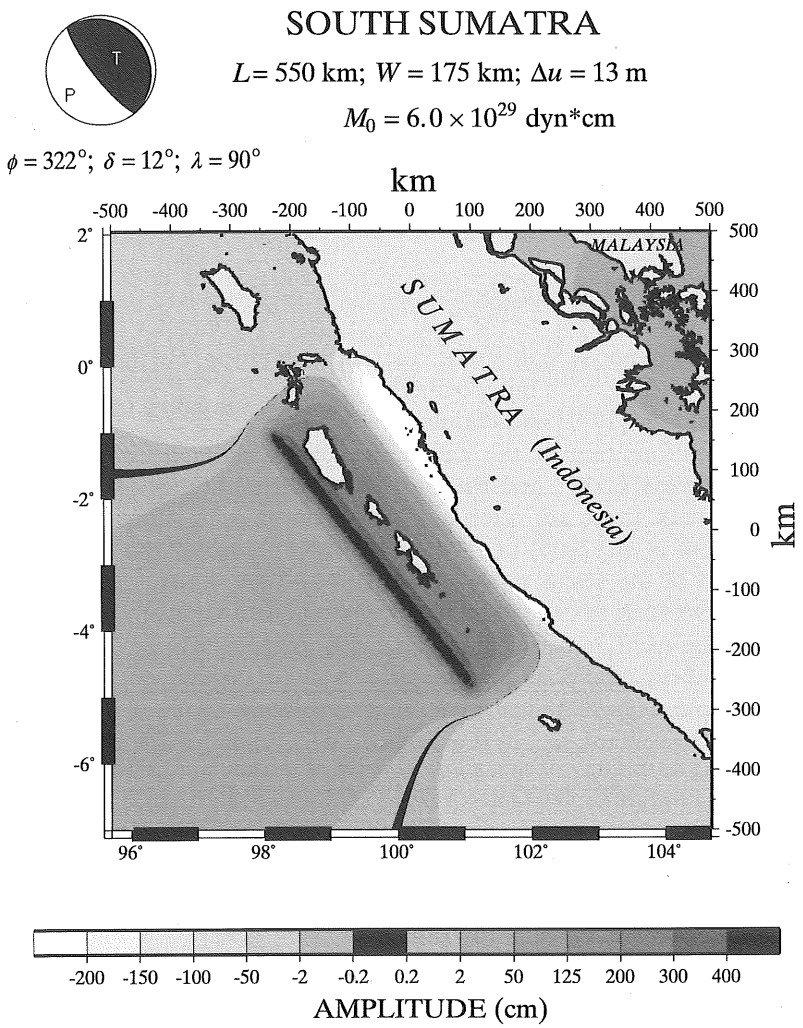

Fig. 5.03 – Field of vertical static displacement u_z computed using *Mansinha and Smylie*'s [1971] algorithm in the scenario of the possible repeat of the 1833 mega-thrust earthquake along the coast of Southern Sumatra. The shallow-dipping thrust fault mechanism is sketched at upper left, and relevant fault parameters listed at the top. The two-dimensional field of u_z values is then interpreted as the initial condition $\eta(t = 0^+)$ of the hydrodynamic simulation shown on Fig. 5-04.

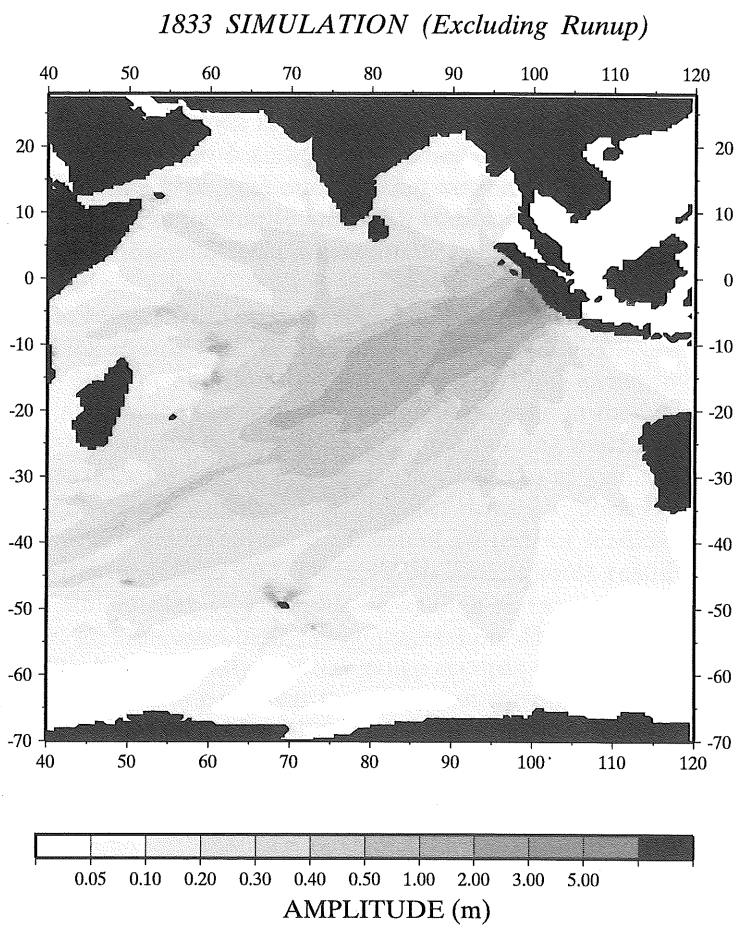

Fig. 5.04 – Maximum tsunami amplitude obtained by simulation of a repeat of the 1833 South Sumatra earthquake, based on the source model of *Zachariasen et al.* [1999]. Note the strong lobe of directivity at right angles to the strike of the fault, and the local focusing effect of shallow bathymetric features such as the Southwest Indian Ocean Ridge or the Kerguelen Plateau. After *Synolakis and Okal* [2006].

An interesting aspect of the field of static displacements presented on Fig. 5-03 is its asymmetry: along a cross-section perpendicular to the fault strike (Fig. 5-05), it features a trough near the coast, and a large hump oceanwards. This results from a combination of factors, namely the thrusting mechanism of the earthquake, the shallow dip angle δ of the fault (taken here as 12°), and the position of the centroid of rupture seawards of the shoreline. These parameters are remarkably robust for the overwhelming majority of the large interplate thrust earthquakes generating most damaging tsunamis, as they simply express the geometry of rupture in the context of the unifying theory of plate tectonics. Since the static displacement field of the rupture constitutes the initial condition of the hydrodynamic problem, *Tadepalli and Synolakis* [1994, 1996] predicted theoretically that the initial waveform of the tsunami should be negative (*i.e.*, a down-draw, or so-called "leading depression") in the direction of the beach, and positive (*i.e.*, a "leading elevation") out at

sea. Thus, the tsunami phenomenon on a nearby coastline should start with a recess of the sea. This was first confirmed during the 1995 tsunami in Manzanillo, Mexico [*Borrero et al.,* 1997], and as summarized by *Synolakis et al.* [2007], widely reported during the Sumatra-Andaman tsunami at shorelines located downdip of the epicenter (Aceh Province, Thailand, Malaysia). By contrast, at distant shores located across the ocean basin from the epicenter (*e.g.,* Sri Lanka), the first oscillation of the tsunami was reported as a leading elevation, as was the first impulse along the JASON satellite profile [*Scharroo et al.,* 2005].

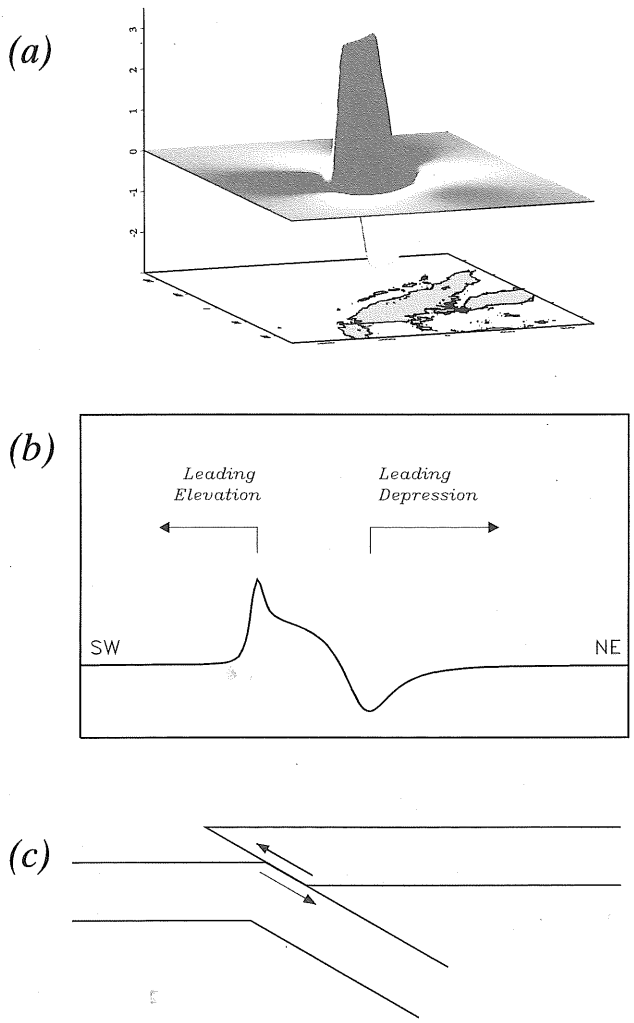

Fig. 5.05 – *(a):* 3-dimensional visualization of the static displacement field shown on Fig. 5-03, looking from East-Southeast. Note the landwards trough generating a leading-depression wave towards Sumatra, and the oceanward hump. *(b):* Cross-section of the static displacement u_z shown on Fig. 5-03, in the azimuth N52°E, *i.e.,* perpendicular to the fault strike. Note the asymmetry of the profile, generating a leading depression towards the shore and a leading elevation towards the high sea. *(c):* Cross-section of co-seismic displacements at a subduction zone, in the plate tectonic framework. Figures not drawn to scale.

The onset of a tsunami as a leading depression wave in the most common geometries involving shorelines at subduction zones provides a natural warning, as the phenomenon starts with its most benign part, namely the recess of the sea, which can serve as a harbinger of the catastrophic elevation to follow. Indeed, this is recognized as a form of warning warranting self-evacuation, in the ancestral traditions of indigenous populations regularly exposed to such cataclysms. However, it should be borne in mind that not all tsunamis are generated by interplate thrust events, and that subduction zones can host large intraplate earthquakes, most often featuring normal faulting (a geometry exactly opposite that of thrust faulting), as the result of the internal rupture of the subducting lithospheric plate. Among them, the events of 1977 in Sumbawa, Indonesia [*Kato and Tsuji,* 1995], and especially 1933 in Sanriku, Japan [*Kanamori,* 1971] generated catastrophic tsunamis, the latter being the second most lethal tsunami in the 20th century, with upwards of 3000 deaths. Because of their normal faulting mechanism, such events should generate tsunamis approaching nearby coastlines as leading elevations, and thus providing no advance notice of inundation. However, observations during the 1977 Sumbawa earthquake reveal a consistent pattern of leading depressions as reported by witnesses [*Kato and Tsuji,* 1995]. This is most readily explained by these authors' simulations, which predict a leading elevation, but of small enough amplitude as to go unnoticed by the local population. This interpretation is upheld by *Abe*'s [1978] detailed study of tidal gauge records of the 1933 Sanriku earthquake, where he shows in particular that the exact waveform of the leading elevation can be very sensitive to the dip angle of the fault. A similar pattern was also observed during the 2004 Sumatra tsunami, this time in the farfield as the earthquake featured a classic underthrusting mechanism.

2.3. *The possible contribution of a horizontal displacement*

In the context described above, a legitimate question can be the possible role, in the generation of the tsunami, of the horizontal motion of the boundaries of the ocean basin during the earthquake. Such motion could be important in the presence of a sloping seafloor above the fault zone. This problem was examined both theoretically and in the laboratory by *Iwasaki* [1982] and *Synolakis* [1986], who concluded that this contribution will generate a sustainable tsunami only for steep slopes, in practice greater than 1/3, a value much larger than typically found on the ocean floor, where even bathymetry described as "steep" rarely exceeds a slope of 10°. However, the limiting case of the horizontal displacement of a vertical wall (which for example would describe a strike-slip fault cutting through an island shore) could lead to a significant local wave at the beach, given a Froude number (*i.e.,* the ratio of fluid particle velocity to the phase velocity of the wave) approaching 1. This could explain the large tsunami observed in the near field at Mindoro, Philippines on 14 November 1994 following a strike-slip earthquake whose fault ran across the island shoreline [*Imamura et al.,* 1995].

In the wake of the 1994 Java "tsunami earthquake", *Tanioka and Satake* [1996*a*] examined the possible contribution to the vertical displacement of water of the horizontal motion of a sloping seafloor, which they suggested could be relatively steep in that area. They concluded that the contribution can affect slightly the

shape and amplitude of the tsunami, but not to the extent of changing its order of magnitude.

3. Tsunamis as free oscillations of the Earth: the normal mode formalism

The simulation algorithm described above suffers from a number of intrinsic limitations due to the simplifying assumptions used in its two steps. On the one hand, the computation of the static deformation ignores the presence of the water layer; on the other hand, the numerical simulation of the tsunami in the water considers a perfectly rigid (hence undeformable) bottom as a boundary condition. It is clear that these two assumptions are mutually exclusive, and thus their separate use in subsequent parts of the modeling is less than satisfactory, although it can be lent some support from *Tinti and Armigliato*'s [1998] demonstration that the static deformation of an elastic half-space is not affected when it is overlain by a liquid half-space. In addition, the model of a homogeneous elastic half-space neglects the possible influence of topography and structural layering on the response of the ocean floor.

In a series of landmark papers, *Ward* [1980, 1981, 1982] has proposed to interpret a tsunami wave as a particular case of the free oscillations of the Earth. Because the spheroidal modes of the planet involve changes in the distribution of mass in its interior, it has been realized since *Love* [1911] that gravity forms part of the restoring force in their oscillations, and that its contribution must be included in their computational algorithms [*e.g., Pekeris and Jarosch,* 1958; *Saito,* 1967; *Wiggins,* 1976]. As a result, the latter handle tsunami modes seamlessly when an appropriate combination of wave number and frequency is targeted, and given a sufficient sampling of the eigenfunction inside the water column.

This approach allows both the consideration of the finite elasticity of the oceanic column (which turns out to be negligible), and the use of a layered structure for the solid Earth, which can be more representative of the source properties of large earthquakes. The eigenfunction of the tsunami mode is no longer limited to the water column, but rather prolonged into the solid Earth, as described on Fig. 5-06. In the ocean, and at a typical period of 1000 s, the energy of the mode remains 99.9% gravitational and only 0.1% elastic, whereas it is mostly elastic (77%) in the solid Earth. The coupling at the ocean bottom results from the [positive] excess pressure caused by an [upwards] deformation η of the sea surface, to which a solid with a finite rigidity μ responds through a [downwards] vertical displacement y_1. In the limit of a low phase velocity C (characteristic of tsunamis), and for a Poisson solid, *Okal* [1988, 1991, 2003] has shown that

$$\frac{y_1}{\eta} = -\frac{3}{4} \cdot \frac{\rho_w g}{\mu k} \tag{4}$$

where ρ_w is the density of water, g the acceleration of gravity, and k the wavenumber of the tsunami. The ratio (4) remains on the order of –0.01 for typical values of μ and k. Even though the ocean bottom is not a welded interface, this vertical deformation y_1 is accompanied by a horizontal component of the eigenfunction in the solid, which is required in order to propagate a viable inhomogeneous wave

through the solid medium with the phase velocity imposed by the tsunami, its amplitude at the interface being $ly_3 = -(1/3)\, y_1$ in the notation of *Saito* [1967]. Both y_1 and ly_3 decay with depth in the solid, with a skin depth approximately equal to the wavelength $\Lambda = 2\pi / k$ of the tsunami [*Okal,* 2003].

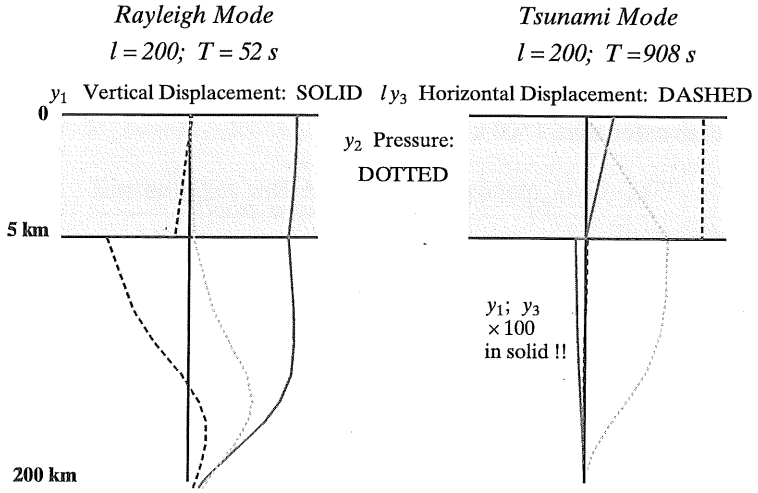

Fig. 5.06. – Variation with depth of selected components of the eigenfunctions of the Earth's free oscillations in the case of a classical Rayleigh mode *(left)* and of a tsunami mode *(right).* In both cases, the angular order is $l = 200$, corresponding to a wavelength $\Lambda \approx 200$ km. The vertical displacement is plotted as the solid line, the horizontal component as the dashed line (on the same scale), and the overpressure as the dotted one (on an unrelated scale). In the case of the tsunami, the scale for displacements has been multiplied by 100 in the solid Earth to make them visible. Vertical scales in the water layer and solid Earth are also different. Note the weak penetration of the tsunami eigenfunction into the solid Earth, and its slow decay with depth.

One of the most seminal aspects of the normal mode formalism is that it simplifies greatly the investigation of tsunami excitation by seismic sources. We recall that *Gilbert* [1970] has shown that the excitation of a free oscillation of the Earth by a point source double-couple $\mathbf{M}$ buried at the location $\mathbf{r}_s$ inside the planet is proportional to the full scalar product $\langle \mathbf{M} : \varepsilon(\mathbf{r}_s) \rangle$ of the moment tensor by the eigenstrain of the mode at the source. In this framework, excitation coefficients expressed in a more familiar geometry related to the physical angles ϕ (strike), δ (dip) and λ (strike) were derived for seismic modes by *Kanamori and Cipar* [1974], and are computed routinely as part of the numerical solution of the free oscillation problem. Such calculations are immediately applicable, with only cosmetic changes to the codes, to the case of tsunami modes [*Ward,* 1980; *Okal,* 1988].

Before detailing the most important results regarding tsunami excitation by seismic sources, we must stress some limitations of the normal mode formalism. First and foremost, normal mode theory considers a laterally homogeneous Earth, or at most can handle a slightly heterogeneous structure [*Madariaga,* 1972; *Woodhouse and Dahlen,* 1978]. Thus, it will not be applicable to the simulation of tsunamis in the near field, where the interaction with the receiving beach is of primordial importance. In addition, seismic normal mode theory has been devel-

oped only as a linear algorithm, and thus will be applicable to tsunamis only when wave amplitudes η are small compared to water depth H and to wavelength Λ. On the other hand, given sufficient vertical sampling of the water column, it can be applied effortlessly outside the shallow-water approximation, in conditions where traditional methods become computationally prohibitive in the far field.

In the general framework of normal mode theory, we now discuss several properties of tsunami excitation; we re-emphasize that they apply only to tsunamis observed in the far field, traditionally defined as extending more than a few wavelengths away from the source, which in the case of large tsunamis, would translate into distances greater than 1500 km.

3.1. *Excitation is always small*

Most importantly, and as shown on Fig. 5-06, the eigenfunction penetrates the solid Earth, but only with very small amplitude. Therefore, and because the excitation is proportional to the eigenstrain at the depth of the source, it remains relatively small. Just like a violinist does not make music by raking the bow near the bridge or the nut where the string cannot move, most earthquakes are fundamentally inefficient at exciting tsunamis, because they do so at what amounts to a node of the eigenfunction. It requires a truly gigantic source to generate a tsunami capable of inundation and destruction, especially in the far field. Synthetic maregrams generated by summation of normal modes suggest only millimetric peak-to-peak amplitudes in the far field on the high seas for a reference moment of 10^{27} dyn*cm [*Ward,* 1982; *Okal,* 1988].

3.2. *Excitation is proportional to M_0*

In the absence of interference effects due to source finiteness and directivity (which will be discussed in Section 5), *Gilbert*'s [1970] theory predicts an excitation growing linearly with seismic moment, like that of all seismic spectral amplitudes unaffected by source finiteness. This is valid only for amplitudes η on the high seas, excluding the response of coastlines and harbors, and as such was for a long time difficult to verify. This is now becoming possible through the direct recording of tsunamis at sea, using the so-called "tsunameters" [*González et al.,* 2005]. In the past, observations at selected harbors known to involve few if any non-linear resonant effects have generally upheld this linearity [*e.g., Talandier and Okal,* 1989].

3.3. *Thresholds; when and where*

The combination of the above two remarks leads to an estimate of $M_0 \geq 5 \times 10^{28}$ dyn*cm for the minimum seismic moment required to generate a transoceanic tsunami inflicting damage in the far field, as a zero-to-peak amplitude of ~10 cm on the high seas is capable of running up to several meters on land. This threshold estimate is generally borne out by observations, and incidentally forms the backbone of decision algorithms at warning centers. In principle, frequency-magnitude relationships, first proposed by *Gutenberg and Richter* [1941] and justified theoretically by *Rundle* [1989], suggest that there should be approximately one such event every five years, but their extrapolation to earthquakes of very great size

suffers from both theoretical limitations [*Okal and Romanowicz,* 1994] and undersampling. In practice, there have been 11 such earthquakes since 1940, listed in Table 1, of which ten were at sea. All tsunamis having inflicted casualties in the far field during that period were generated by six of those ten events, which confirms the validity of the above threshold as a necessary, if not sufficient, condition. We note further that eight of the 11 events in Table 1 occurred within a 19-yr interval between 1946 and 1965, which expresses the well-known fluctuations in seismic moment release over the past few decades.

TABLE 1.
Earthquakes with $M_0 \geq 5 \times 10^{28}$ dyn*cm, 1940–2007

Region	Date D M (J) Y	M_0 (10^{27} dyn*cxm)	Reference	Tsunami death toll in near and far field
Aleutian	01 APR (091) 1946	85	a	Near field sparsely populated: 5 deaths Far field: 161 deaths
Assam	15 AUG (227) 1950	140	b	Continental; no tsunami
Kamchatka	04 NOV (309) 1952	230	b,c,d	Near field: 2000–14000 deaths Far field: Damage strong in Hawaii; no deaths
Aleutian Is.	09 MAR (068) 1957	> 200	b,e,f	No fatalities reported despite large run-up in both near and far field
Chile	22 MAY (143) 1960	5000	g	Near field: 1000+ deaths Far field (Hawaii, Japan): 200+ deaths
Kurile Is.	13 OCT (286) 1963	75	h,i	No reported deaths or far-field damage
Alaska	28 MAR (088) 1964	820	j	Near field: 106 deaths Far field (Western US): 17 deaths
Rat Island	04 FEB (035) 1965	125	k,l	No deaths in near or far field
Sumatra-Andaman	26 DEC (261) 2004	1150	m	Near field (Aceh): 220,000 Far field: 60,000
Nias-Simeulue	28 MAR (087) 2005	105	n	No fatalities due to tsunami
Bengkulu, Sumatra	12 SEP (255) 2007	55	o	No fatalities due to tsunami

References. a: *López and Okal* [2006]; b: *Okal* [1992]; c: *Kaistrenko and Sedaeva* [2001]; d: *Macdonald and Wentworth* [1954]; e: *Johnson et al.* [1994]; f: *Fraser et al.* [1959]; g: *Cifuentes and Silver* [1989]; h: *Kanamori* [1970*a*]; i: *Solov'ev* [1965]; j: *Kanamori* [1970*b*]; k: *Wu and Kanamori* [1973]; l: *Hwang et al.* [1972]; m: *Tsai et al.* [2005]; n: *McAdoo et al.* [2006]; o: *Borrero et al.* [2007].

Until 2004, it was generally thought, following *Ruff and Kanamori* [1980], that the maximum expectable earthquake at a subduction zone could be predicted on the basis of two simple parameters (age of subducting lithosphere and rate of convergence), leading to the concept of "safe" subduction zones, from which transoceanic tsunamis would not be generated. Unfortunately, the 2004 Sumatra-Andaman earthquake violated this paradigm, and the re-examination of an updated Ruff-Kanamori dataset has led *Stein and Okal* [2007] to the precautionary conclusion that all sufficiently long subduction zones ($L > 500$ km) must be considered potential sources of mega-thrust earthquakes.

In the near-field, it is more difficult to define a universal moment threshold for a damaging tsunami, which may depend on local conditions. Shallow events ($h \leq 70$ km) with $M_0 \geq 10^{27}$ dyn*cm occurring in the vicinity of coastlines will generally result in tsunamis with run-ups of metric amplitude, but smaller events can occasionally be tsunamigenic. Also, the inflicted damage reflects the density of local population and infrastructure. For example, the considerable local run-up (reaching 21 m on Matua) from the earthquakes of 15 November 2006 and possibly 13 January 2007 (M_0 = 3.4 and 1.7 $\times$ 10^{28} dyn*cm, respectively) was not documented before a surveying team landed on the uninhabited Central Kuril Islands in August 2007 [*Bourgeois et al.,* 2007]. On the average, worldwide historical records show 2 tsunamis per year inflicting damage in the near field.

3.4 Influence of source depth

The relatively slow decay of the eigenfunction with depth, illustrated on Fig. 5-06, predicts that source depth should not be a major parameter in the excitation of far-field tsunamis by earthquakes, at least in the range 10–100 km. *Okal* [1988] has given a detailed justification of this arguably paradoxical remark, using both frameworks—normal modes and classical gravity theory. In this respect, several examples deserve mentioning, such as the 1977 Tonga earthquake, whose tsunami amplitude (12 cm peak-to-peak at Papeete) was not deficient given its moment of 1.4 to 2.0 $\times$ 10^{28} dyn*cm [*Talandier and Okal,* 1979, 1989], despite a centroid depth later estimated at 100 km [*Lundgren and Okal,* 1988], and the recent event on 03 May 2006, also in Tonga (1.1 $\times$ 10^{28} dyn*cm; centroid depth 68 km), whose tsunami reached 25 cm peak-to-peak in Papeete [*O. Hyvernaud,* pers. comm., 2006] and 1.2 cm on a tsunameter off the coast of Oahu [*Tang et al.,* 2006].

3.5. Crustal structure

On the other hand, crustal stratification, shown by *Okal* [1982] to have little effect on the dispersion of tsunamis, can affect their excitation when the source is located, even partially, in a "sedimentary" layer featuring low rigidity [*Okal,* 1988]. This situation could contribute to the enhanced tsunami excitation for events occurring on splay faults rupturing through an accretionary prism, such as the "tsunami earthquakes" (see below) of 1975 in the Kuriles or 1896 off the coast of Sanriku [*Fukao,* 1979; *Tanioka and Satake,* 1996*b*].

3.6. Focal geometry

The question of the dependence of tsunami excitation on the focal geometry of the earthquake has long been controversial. Common wisdom would suggest that strike-slip earthquakes produce little if any vertical deformation of the ocean floor, and as such should not be efficient tsunami generators. This is contradicted by the structure of the eigenfunction plotted on Fig. 5-06, which predicts a ratio as large as 1/3 between the horizontal and vertical components of displacement at the top of the solid medium and, in turn, comparable values for the excitation coefficients characteristic of strike-slip and 45° faults ($l^2 K_2/K_0 \approx 1$ in the notation of *Kanamori*

and Cipar [1974]) [*Okal,* 2003]. The origin of this paradox lies in the need, under the classical gravity wave formalism (Fig. 5-03), to integrate contributions of the vertical displacement over the whole source area (formally over the entire ocean floor), which forbids any quick intuitive conclusion regarding the far-field tsunami. In particular, for any source of finite dimension, algorithms such as *Mansinha and Smylie*'s [1971] or *Okada*'s [1985] do predict poles of accumulation of vertical displacements localized in the vicinity of the tips of a strike-slip fault. They express the strong perturbation of the field of released strain in those areas, which is necessary to ensure the material's cohesion along a continuous path from one side of the fault to the other, around the fault tip. In this respect, it is worth noting that the large strike-slip event of 23 December 2004 near Macquarie Island generated a tsunami recorded in the far field by a seismic station located on the Ross Ice shelf along the coast of Antarctica, in a geometry approaching that of a tsunameter detection of the wave on the high seas [*Okal and MacAyeal,* 2006].

3.7. Energy of a tsunami generated by an earthquake

As detailed in *Okal* [2003] and summarized in the Appendix, the energy transferred from the seismic source to the tsunami can be computed from normal mode theory, and reconciled with its more classical derivation [*Kajiura,* 1981], the latter based essentially on the sketch on Fig. 5-02. The most remarkable aspect of these results is that the energy of the tsunami grows like $M_0^{4/3}$, *i.e.,* faster than the seismic moment, and hence than the total energy released at the source, expressed by the product $M_0 \cdot \varepsilon_{max}$. This is to say that larger earthquakes transfer an increasingly large fraction of their energy to the tsunami. However, this fraction remains in all cases very small (at most 1.3% in the case of the 1960 Chilean earthquake, the largest one ever measured instrumentally), and would reach clearly irrational values of 1 or greater only for a fault length equivalent to the Earth's circumference, a scale on which scaling laws have long ceased to be applicable. Another interesting aspect of the formulæ given in the Appendix is that the total energy fed into the tsunami, E_T, does not depend on the depth H of the water column. This is implicit from the sketch on Fig. 5-02. However, the actual amplitude of the wave in the far field can indeed be depth-dependent, as it follows the repartition with frequency of the total energy computed by *Kajiura* [1981] or *Okal* [2003]. In particular, once a tsunami is generated with a given total energy, and propagates over irregular bathymetry, the resulting amplitude in the far field will be affected by the details of the bathymetry over its source and path. This explains why tsunamis occurring in deeper, rather than shallower, water are eventually more damaging in the far field, as recently verified numerically by *Synolakis and Okal* [2006]. It also accounts partially for the deceptively low far-field tsunami generated by the "second" Sumatra event, the Nias-Simeulue earthquake of 28 March 2005, despite its large moment $M_0 = 1.05 \times 10^{29}$ dyn*cm, as its epicentral area involved much shallower bathymetry than that of the 2004 event. In addition, and as pointed out by *Synolakis and Arcas* [quoted by *Kerr,* 2005], the presence of large islands above the fault zone significantly reduced the amount of water available to be displaced and generate the tsunami.

3.8. *A tsunami magnitude scale:* M_{TSU}

The possibility of assigning a magnitude to an earthquake based on the amplitude of its tsunami was investigated by *Abe* [1983, 1989], who proposed a scale M_t using instrumentally measured tsunami amplitudes. This approach, derived mainly for the near field, remains empirical, and M_t has no theoretically derived relation to M_0. In addition, until recently, the only instruments capable of measuring the amplitude of tsunamis were tidal gauges; the interpretation of their records is hampered by the complexity of the response of coastlines, bays and harbors, where most of these devices are located, and by their intrinsic mechanical non-linearity.

On the other hand, the linearity derived from normal mode theory between the amplitude of a tsunami mode (and hence of the whole wave) and the seismic moment of the parent earthquake opens the possibility of developing a tsunami magnitude directly related to M_0, and fully justified from the theoretical standpoint. With the advent of tsunameters directly measuring the tsunami by recording its overpressure on the ocean bottom [*González et al.,* 1991; 2005], and to a lesser extent of direct measurements of tsunamis using satellite altimetry [*Okal et al.,* 1999; *Scharroo et al.,* 2005; *Kulikov et al.,* 2005], it is now possible to eliminate nonlinear difficulties at the shorelines, and to measure the tsunami directly on the high seas. In this framework, *Okal and Titov* [2007] have developed a tsunami magnitude M_{TSU} , inspired from the mantle magnitude M_m introduced for long-period Rayleigh waves by *Okal and Talandier* [1989], and directly related to M_0 through

$$M_{TSU} = \log_{10} M_0 - 20 = \log_{10} X(\omega) + C_S + C_D + C_0 \qquad (5)$$

where $X(\omega)$ is the spectral amplitude of the tsunami at angular frequency ω, C_D a distance correction expressing geometrical spreading on the spherical Earth, C_S a source correction depending only on ω and derived form normal mode theory, and C_0 a locking constant depending on the nature of the observable X (amplitude η at the surface or overpressure p at the ocean floor), and also fully justifiable on theoretical grounds. All details can be found in *Okal and Titov* [2007].

This concept was successfully applied to five tsunamis recorded by the growing network of tsunameters. As none were deployed in the Indian Ocean at the time of the 2004 Sumatra-Andaman tsunami, *Okal and Titov* [2007] processed the trace from the JASON satellite altimeter (allowing for its specific character of being neither a time nor a space series). Fig. 5-07 shows that the M_{TSU} algorithm recovers the seismic moment satisfactorily, even in conditions where the concept should not be applicable, such as the great circle path crossing a continental mass. In addition, *Okal* [2007*a*] has shown that the concept can be applied to seismic records of tsunami waves obtained at island or continental stations.

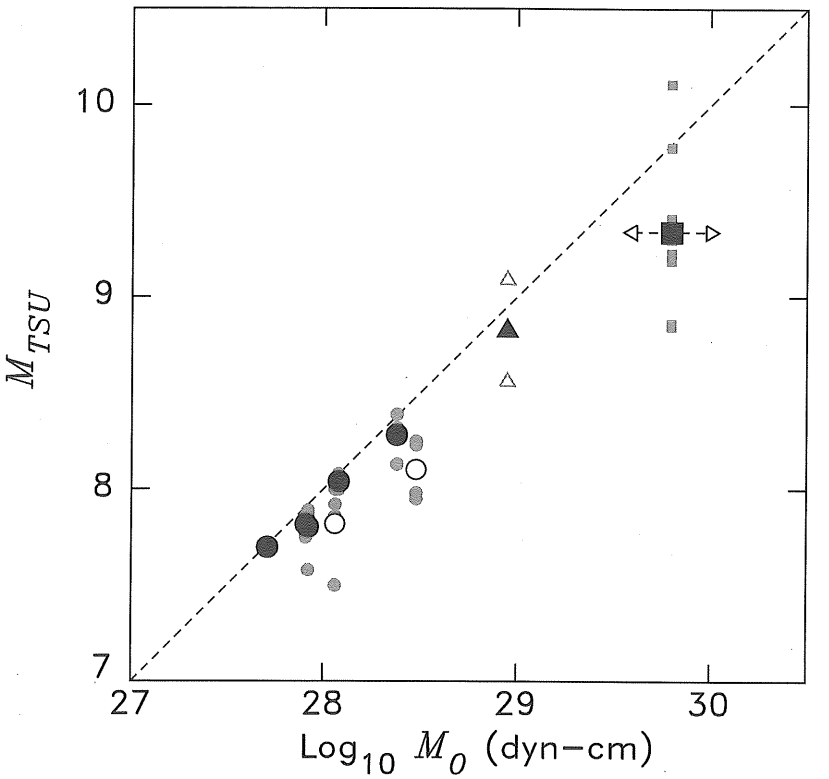

Fig. 5.07 – Performance of the magnitude M_{TSU} studied for recent tsunamis, as a function of the published moment M_0. For each earthquake, the small gray dots are the individual measurements at each tsunameter, averaged over usable frequencies. The large symbol is the value averaged over all tsunameters. The two open symbols refer to events for which the great circle paths intersect either a continent or the Aleutian arc. The square symbols are for the JASON satellite profile of the 2004 Sumatra-Andaman tsunami, with the horizontal arrows indicating the range of published moments. The triangles refer to the 1946 Aleutian event and are virtual measurements made on synthetic maregrams computed by *Okal and Hébert* [2007]. See *Okal and Titov* [2007] for details.

3.9. The high-frequency components of the tsunami wave

Because it works seamlessly without special assumptions outside the domain of validity of the shallow-water approximation ($k \cdot H << 1$), normal mode formalism is particularly well suited to investigate the higher-frequency components of tsunamis, typically in the 2–10 mHz frequency band. Since they are strongly dispersed according to the classical formula

$$\omega^2 = g\, k \cdot \tanh\,(k \cdot H) \tag{6}$$

such components arrive both later and with a smaller amplitude than the lower-frequency (and conventional) part of the tsunami spectrum (typically 0.3–1 mHz). However, during surveys of the 2004 Sumatra tsunami in Réunion and Madagas-

car, *Okal et al.* [2006*a,b*] have reported occurrences of large vessels breaking their moorings in harbors several hours after the arrival of the tsunami; these phenomena were interpreted by the resonance of harbor basins under the delayed high-frequency components of the tsunami [*Pančošková et al.,* 2006]. As they carry obvious implications in terms of tsunami warning and civil defense, it is imperative to understand to which extent such effects can be predicted and quantified. In this respect, *Okal et al.* [2007] have used records of the 2004 tsunami on hydrophones of the Comprehensive Nuclear-Test Ban Treaty Organization to show that its high-frequency spectral amplitudes can be successfully quantified from the seismic moment of the earthquake, using normal mode theory.

3.10. Tsunamis in the atmosphere and above

The argument used to justify the continuation of the tsunami eigenfunction into the solid Earth is also applicable at the other boundary of the oceanic column, namely the sea surface. In all above computations, the latter is taken as a "free" boundary where pressure must vanish, but it is really overlain by an atmosphere "only" 1000 times less dense than water. Accordingly, the tsunami mode is actually continued upwards in the form of a gravitational oscillation of the atmosphere. This idea of treating various scenarios of coupling between the solid, liquid and gaseous layers of the Earth as the propagation of a single wave through a combined structure was pioneered by *Haskell* [1951] and developed by *Harkrider et al.* [1974] for the conjugate problem of the generation of seismic Rayleigh waves by atmospheric explosions. While the energy density of the mode continued into the atmosphere is expected to decrease with height, the concurrent rarefaction of the material density $\rho_{atm.}$ results in an actual *increase* of the particle displacement with altitude, the amplification of sea-surface disturbances reaching up to 5 orders of magnitude at the base of the ionosphere. This concept, observed for Rayleigh waves by *Yuen et al.* [1969] was predicted for tsunamis by *Peltier and Hines* [1976], and first observed by *Artru et al.* [2005] through the disruption of GPS signals over Japan during the 2001 Peruvian tsunami; it was modeled quantitatively in the case of the 2004 Sumatra tsunami by *Occhipinti et al.* [2006]. It could bear some potential for real-time detection of tsunamis over non-instrumented portions of the ocean basins, using various space-based technologies.

4. Earthquake tsunamis in the near field: Scaling laws and invariants

In general, the run-up of a tsunami on a local beach following an earthquake will be controlled by a very large number of parameters, comprising those describing the earthquake source (seismic moment and geometry), its physical environment (earthquake depth, bathymetry of the source area), and the properties of the receiving shore line (above- and below-sea level topography of the beach, presence of bays, harbors, estuaries, etc.). Successful simulations can be run only on a case-by-case basis taking into account all specific parameters. Nevertheless, it is desirable to understand which of them can define trends, and if possible robust invariants.

In this general framework, one notes the linearity of the Somigliana tensor, which is carried into the algorithm of *Mansinha and Smylie* [1971] described in Section 2, suggesting that, everything else being equal, the excitation of the tsunami should grow linearly with the slip on the fault plane, Δu, and so should the final run-up ζ on the shore, in the simplified model of an ocean-beach-shore system offering translational symmetry, and for moderate amplitudes precluding the development of non-linearities. Similarly, the lateral extent of the inundation by the tsunami should be expected to grow like the dimension L of the fault over which the rupture takes place. These simple arguments then suggest that the aspect ratio of the distribution of run-up along the beach should express the ratio $\Delta u / L$, and hence the strain ε released by the dislocation, known to be, at least in principle, an invariant of the seismic source.

Motivated by this remark, *Okal and Synolakis* [2004] have considered the idealized model of an earthquake source occurring offshore of a perfectly linear beach (Fig. 5-08*a*), and studied the field of run-up ζ along the direction y of the waterfront. Their simulations used the MOST code, for a very large number of scenarios obtained by varying the scalar moment M_0 of the earthquake, the three angles ϕ, δ, λ of its focal geometry, the distance D of the earthquake from the shore, its hypocentral depth h, the thickness H of the oceanic column at the source, and the slope β of beach. For each case under study, they fit the distribution of run-up with a bell-shaped curve of the form

$$\zeta(y) = \frac{b}{\left(\frac{y-c}{a}\right)^2 + 1} \tag{7}$$

and focus on the two dimensionless parameters $I_1 = b/\Delta u$ and $I_2 = b/a$. As detailed in *Okal and Synolakis* [2004], both I_1 and I_2 are found to be robust, and thus play the role of invariants in this study. Most importantly, and as shown on Fig. 5-08, they feature upper bounds (respectively 1.35 and 7×10^{-5} in the numerical experiments), clearly controlled by the properties of the seismic sources and its own invariants. By contrast, a similar study using representative models of submarine landslides produced much steeper distributions of run-up along coastlines, with aspect ratios I_2 always remaining greater than 10^{-4} (Fig. 5-08*c*).

These theoretical predictions were upheld by fitting profiles of the form (7) to run-up datasets documented during field surveys following the major tsunamis of 1985–2001 [*Synolakis and Okal,* 2005] (allowing for a slight increase of I_1 to a maximum value of 2, in view of our imprecise experimental knowledge of Δu). Among all earthquakes tested, the only two clearly violating the pattern are the 1998 Papua New Guinea and 1946 Aleutian events, whose local tsunamis are explained through the triggering of major underwater landslides.

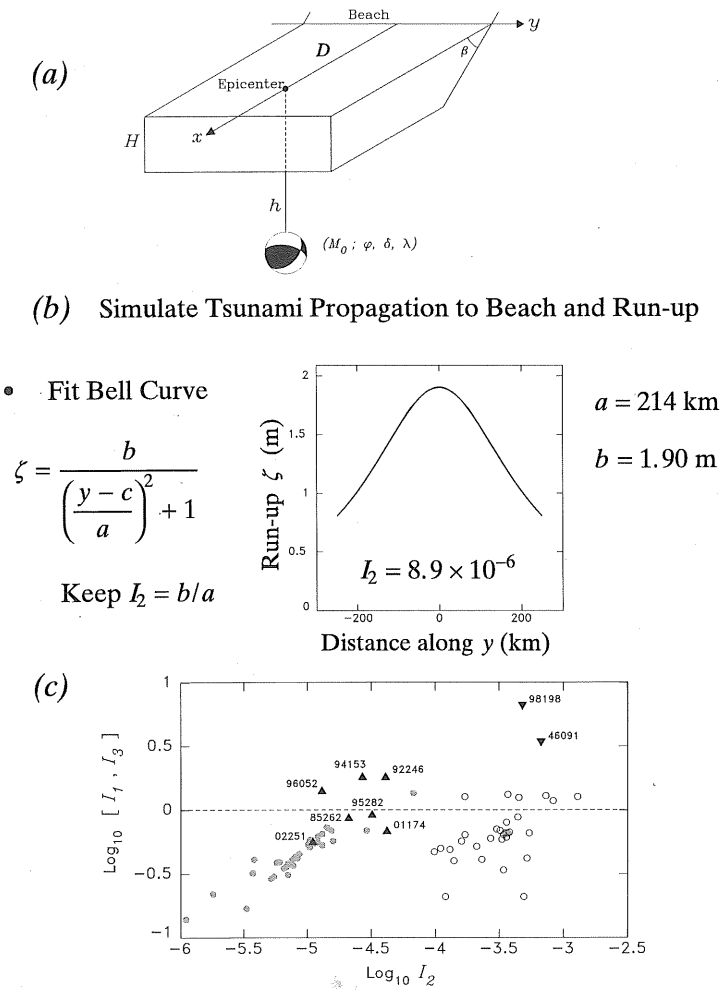

Fig. 5.08 – Scaling invariants for earthquake sources in the near field, after *Okal and Synolakis* [2004]. *(a)* Sketch of the geometry considered, with parameters varied in numerical experiments. *(b)* Run-up ζ at the beach plotted as a function of coordinate *y*, fitted with a bell-shaped curve of aspect ratio I_2. *(c)* Logarithmic plot of $I_1 = b/\Delta u$ as a function of I_2 for a large population of dislocation sources (solid gray dots). Note the bounds on both quantities. By contrast, the open symbols refer to dipolar sources modeling landslides, and the ordinate is then $\log_{10} I_3$, the ratio of *b* to the depth of the trough in the initial dipole. Note that the two populations are separated at the $I_2 = 10^{-4}$ threshold. The triangles denote the aspect ratios of the distributions of runup surveyed after recent tsunamis (identified by Julian date). The only clear violators of the bounds $I_1 < 2$; $I_2 < 10^{-4}$ are the 1998 Papua New Guinea and 1946 Aleutian earthquakes, whose local tsunamis were due to landslides.

In the case of the 2004 Sumatra-Andaman earthquake, postdating *Okal and Synolakis'* [2004] study, the parameter I_2 cannot be adequately studied, as a continuous coastline does not parallel the full extent of the fault rupture. On the other hand, regarding I_1, we note a maximum surveyed run-up of 31 m at Lhoknga (discounting splashes on vertical cliffs) [*Borrero,* 2005]. As large as this figure can seem, it remains within the bounds of I_1, given estimates of Δu reaching for example up to 19 m on specific segments of the fault plane, in the model of *Banerjee et*

al. [2007]. Thus, near-field run-up during the 2004 Sumatra-Andaman tsunami is accountable within the framework of seismic scaling laws, with a regular, if of course exceptionally large, seismic source, and does not require ancillary phenomena such as catastrophic underwater landslides, or the activation of substantial splay faults.

Finally, *Okal and Synolakis'* [2004] results underscore the value of field survey data acquired in the aftermath of tsunamis, which can give insight into the mechanism of generation of the tsunami through the application of robust discriminants. In turn, the "Plafker rule of thumb (*"Run up on a straight beach* [unaffected by river valleys, bays or harbors] *shall not exceed twice the amount of slip on the fault"*) can be applied as a gross, zeroth-order estimate of expectable local inundation during future tsunamis.

5. Earthquake tsunamis in the far field: Directivity

It has long been known that transoceanic tsunamis feature very strong *directivity, i.e.,* that the amplitude of their waves is a strong function of the azimuth of their path from the parent earthquake. For example, the 2004 Sumatra-Andaman tsunami was particularly destructive in Sri Lanka [*Goffe et al.,* 2006] and Somalia [*Fritz and Borrero,* 2006], but relatively benign at similar or shorter distances in Western Australia. The origin of this effect, lies in the spatial extent of the source, which results, in the far field, in a destructive interference of the waves generated by its individual components, in all azimuths except in the direction perpendicular to the strike of the fault.[2] It was investigated for standard seismic surface waves by *Ben-Menahem* [1961], and applied to tsunamis by *Ben-Menahem and Rosenman* [1972]. For a source with a fault length L rupturing at velocity V_R, spectral amplitudes at angular frequency ω must be multiplied by a directivity function

$$DIR = \left| \frac{\sin X}{X} \right| \quad \text{with} \quad X = \frac{\omega L}{2C} \cdot \left(\frac{C}{V_R} - \cos\psi \right) \tag{8}$$

where C is the phase velocity of the wave, and ψ the azimuth of the path measured from the fault strike. Note that $DIR = 1$ only for $X = 0$; otherwise, $DIR < 1$, expressing destructive interference. Directivity patterns are expected to be sharply different for seismic waves and tsunamis. For the former, the rupture velocity V_R (typically 3.5 km/s) is only slightly less than the typical phase velocity of a Rayleigh wave (C = 4 km/s), and X will be smallest (and consequently DIR largest, approaching 1) for $\psi = 0$, in the direction of propagation of rupture. On the other hand, for tsunamis, the phase velocity C is much less than V_R (typically 1/15, but still 1/5 in the case of the slow rupture of a "tsunami earthquake"), and X vanishes for an angle ψ close to $\pi/2$, meaning that the directivity lobe is directed at right angles from the fault. The physical interpretation of this result is that the faulting

[2] Directivity is superimposed on the radiation pattern expressing the azimuthal variation of excitation from a point-source moment tensor as a function of its focal geometry which, for tsunamis, is usually dominated by an isotropic term in the case of dipping fault planes [*Okal,* 1988, 1991].

takes place instantaneously compared to the propagation times of the tsunami, and therefore that the interference between waves coming from the various elements of the source can be constructive only if the distances traveled are stationary, which is the case in the far field for $\psi = \pi/2$. It also follows from (8) that directivity lobes are narrower for tsunamis than seismic surface waves, and that their width decreases with increasing earthquake size [*Okal and Talandier,* 1991]. Theoretical examples of tsunami directivity functions are presented in Fig. 5-09*a,* and the case of the 2004 Sumatra-Andaman event is illustrated conceptually on Fig. 5-09*b* with a numerical simulation given on Fig. 5-10. It explains for example the relatively moderate amplitudes reported in Madagascar and the Mascarene Islands [*Okal et al.,* 2006*a,b*], as opposed to Somalia [*Fritz and Borrero,* 2006].

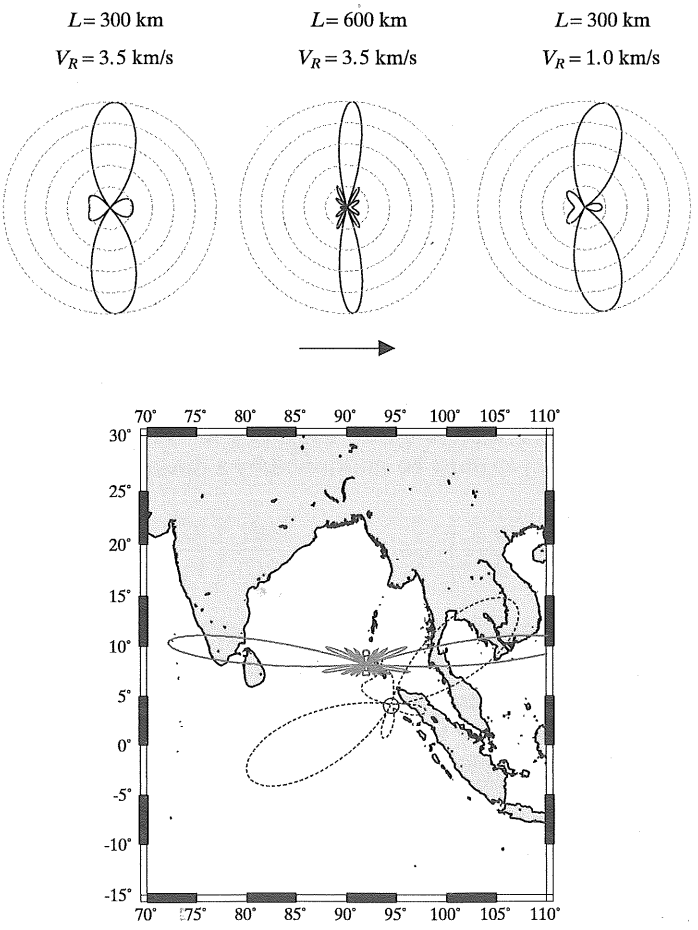

Fig. 5.09 – *Top:* Theoretical azimuthal directivity functions (8) of tsunami waves computed for typical earthquake source scenarios. In all cases, the fault strike is taken along the x axis, as indicated by the arrow. The dashed lines are drawn from DIR = 0.2 (innermost) to DIR = 1(outermost) in steps of 0.2 units. Note the narrowing of the lobe with increasing fault length, and its direction essentially at right angles to the fault. The plot at right represents a slow-rupturing "tsunami earthquake". *Bottom:* Application to the case of the 2004 Sumatra-Andaman earthquake. The solid line represents the directivity function for a 1000–km fault rupturing to the North and centered at 7°N, the dotted one for the model proposed initially, extending only 350 km at an azimuth of 327°, off the coast of Sumatra.

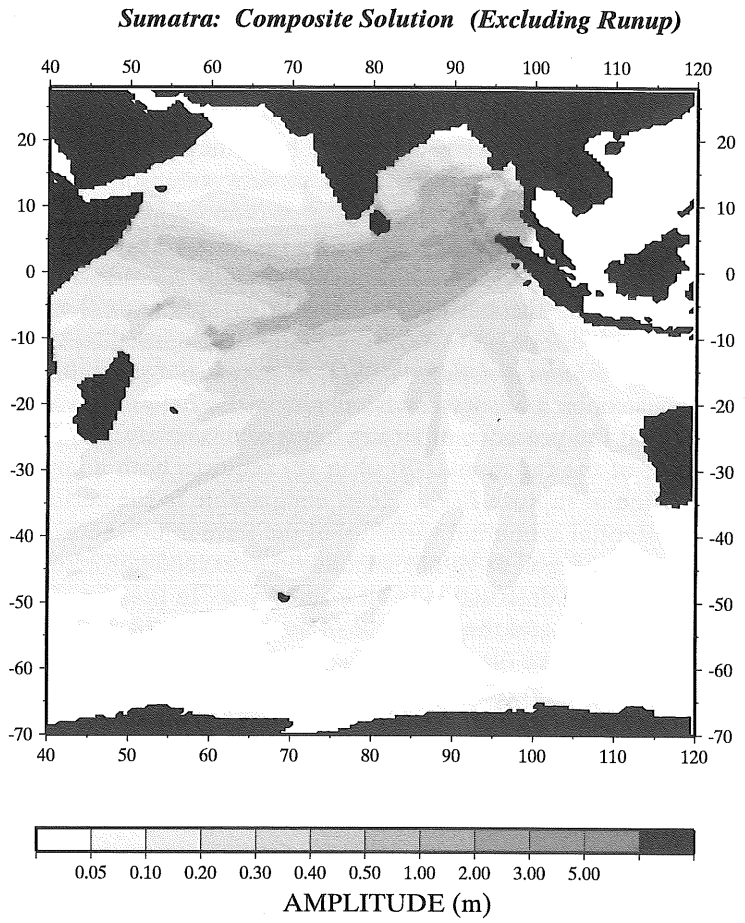

Fig. 5.10 – Same as Fig. 5-04 for the 2004 Sumatra-Andaman tsunami, modeled using the composite seismic source of *Tsai et al.* [2005], extending along the curved arc from Aceh to the Northern Andaman Islands. Note the directivity lobe at right angles to the average direction of rupture. This diagram explains the enhanced amplitudes in Sri Lanka and Somalia, as compared to Western Australia and Madagascar. After *Synolakis and Okal* [2006].

The concept of directivity leads to simple and robust results regarding the relative vulnerability of distant shores to transoceanic tsunamis. For example, as a gross approximation, the Pacific Basin can be taken as circular with plate boundaries tangent to its circumference, and Hawaii at its center. This suffices to explain the repeated disastrous amplitudes in Hawaii from sources as diverse as Chile (1960, which also inflicted death and damage to Japan but largely spared Mexico or California), Unimak (1946, which spared California and South America), or Kamchatka (1952, which spared Japan or California). The exception would be the great 1964 earthquake in Alaska, where the plate boundary striking N66°E strongly departs from this simple model. As a result, the 1964 tsunami spared Hawaii, but was directed at Northern California, inflicting heavy damage and 11 deaths in the community of Crescent City. An important aspect of the directivity

concept is that the azimuth of long faults is well known in the context of plate tectonics, and thus the azimuths of the so-called "swaths of death" featuring maximum tsunami risk in the far field can be predicted in advance.

In addition to source directivity, the amplitude of a tsunami in the far field can also be affected by propagation over irregular bathymetry. In particular, because the velocity of a tsunami, $C = \sqrt{gH}$ under the shallow water approximation, varies with the depth H of the water column, a zone of reduced bathymetry (ridge, plateau) can act as an optical lens and focus the energy of the wave [*Woods and Okal,* 1987; *Satake,* 1988]. This effect, identifiable on Fig. 5-04, is not related to the excitation of the tsunami by the earthquake, and thus transcends the scope of this Chapter. Because it does not grow with source size (as opposed to the focusing by source directivity; *Okal and Talandier* [1991]), it remains of secondary importance in the case of catastrophic transoceanic tsunamis.

Finally, note that the presence of strong lobes of directivity, *i.e.,* a strong variation with azimuth of the function $DIR(\psi)$ in (8) requires both a large value of X (and thus a duration of rupture L/V_R at least comparable to the period of the wave $2\pi/\omega$), and a substantial azimuthal variation of the term in brackets, $(C/V_R - \cos\psi)$. This excludes cases where $C \gg V_R$, corresponding to exceedingly slow ruptures for which the interference is destructive in all azimuths ψ. In practice, this is the case for submarine landslides, and the existence of a strong lobe of directivity in the far field can be used as a source discriminant in this respect, for example in the case of the 1946 Aleutian tsunami [*Okal et al.,* 2002; *Okal,* 2003].

6. The case of "tsunami earthquakes"

This special class of earthquakes was defined by *Kanamori* [1972] as events whose tsunamis are greater than would be expected from their magnitudes, especially conventional ones. In this context, it is worth repeating that *"tsunami earthquakes"* are not to be confused with earthquakes merely generating a tsunami, which are simply referred to as "tsunamigenic". "Tsunami earthquakes" are obvious violators of scaling laws and we now understand that they generally involve a slower than expected rupture, which results in strongly destructive interference patterns for the higher-frequency seismic waves on which conventional magnitudes are measured: 1–s body waves for m_b and 20–s surface waves for the "Prague" magnitude M_s. In the case of particularly slow events, even seismic moments obtained in their immediate aftermath from automated centroid moment tensor inversions can be underestimated as they are derived from mantle surface waves typically in the 100–200 s range. By contrast, the excitation of tsunami waves, typically in the 1000–s period range, involves the full seismic moment, integrated over a much longer time.

"Tsunami earthquakes" can be particularly tragic in the near field where little time is available for a centralized warning and where efficient mitigation relies on self-evacuation of the coastal populations upon their feeling the earthquake. An event lacking high frequencies will produce minimal accelerations resulting in little if any damage to structures, and may even go unnoticed by humans. Such was the case of the great Sanriku, Japan earthquake of 15 June 1896, which was felt along the coast at a weak intensity not exceeding MM IV, but was followed by a devastating tsunami with run-up of 30 m, killing more than 27,000 people [*Kanamori,*

1972; *Solov'ev and Go,* 1984]. On a smaller scale, similar scenarios of tsunami devastation in the near field along sections of coast line where the earthquake *had not even been felt* were reported during the recent "tsunami earthquakes" in Nicaragua (02 September 1992), Java (02 June 1994 and 17 July 2006) and Chimbote, Peru (21 February 1996) [*Abe et al.,* 1993; *Tsuji et al.,* 1995*a; Bourgeois et al.,* 1999; *Fritz et al.,* 2006*a*]. It is clear that such events pose a special challenge to the warning community, as it is imperative to recognize their anomalous character in real-time, in order to issue a warning to populations who may not suspect danger. Table 2 gives a list of documented "tsunami earthquakes". The two earthquakes listed as "probable" are aftershocks of major interplate thrust events, which generated locally catastrophic tsunamis featuring in both instances greater run-up heights than those of the main shocks, despite clearly lower seismic magnitudes. However, in the absence of detailed seismological studies of these ancient earthquakes, it is difficult to formally establish the properties of their sources.

TABLE 2.
Parameters of "tsunami earthquakes", 1896–2006

Origin	Date D M (J) Y	m_b	M_s†	Moment M_0 (10^{27} dyn*cm)	Θ	Tsunami Fatalities	Reference
			Documented				
Sanriku, Japan	15 JUN (167) 1896		7.2	12		27,000	a,b
Unimak, Aleutian Is.	01 APR (091) 1946		7.4	85	–7.0	166	a,c
Northern Peru	20 NOV (325) 1960		6.75	2.7	–6.13	13	d
Kuriles	20 OCT (293) 1963		6.8	7.5	–6.42		e,f
Kuriles	10 JUN (161) 1975	5.8	7.0	0.8	–6.43		e,f
Tonga	19 DEC (353) 1982	5.9	7.7	2.0	–5.76		g,h
Nicaragua	02 SEP (246) 1992	5.3	7.2	3.4	–6.30	160	d,i
East Java	02 JUN (153) 1994	5.7	7.2	5.1	–6.03	223	d,i
Chimbote, Peru	21 FEB (052) 1996	5.8	6.6	2.2	–6.00	12	d,i
Sumatra-Andaman	26 DEC (361) 2004	7.2	8.1	1100	–5.89	280,000	j,k
Central Java	17 JUL (198) 2006	6.1	7.7	4.6	–6.13	668	l
			Probable				
Kamchatka	13 APR (103) 1923		7.2			23	m,n
Cuyutlan, Mexico	22 JUN (174) 1932		6.9			75	o

†Note that magnitudes M_s are not systematically catalogued before 1968. Earlier values are estimates from individual researchers.

References. a: *Kanamori* [1972]; b: *Tanioka and Satake* [1996*b*]; c: *López and Okal* [2006]; d: *Okal and Newman* [2001]; e: *Okal et al.* [2003]; f: *Fukao* [1979]; g: *Okal and Talandier* [1989]; h: *Newman and Okal* [1998]; i: *Polet and Kanamori* [2000]; j: *Stein and Okal* [2005]; k: *Choy and Boatwright* [2007]; l: *Reymond and Okal* [2006]; m: *Menyaĭlov* [1946]; n: *Solov'ev and Ferchev* [1961]; o: *Farreras and Sanchez* [1991].

While most regular earthquake sources feature ruptures propagating along the length of the fault at V_R = 3 to 3.5 km/s, detailed seismological studies of "tsunami earthquakes" have revealed smaller values, reaching as low as V_R = 1 km/s [*Polet and Kanamori,* 2000; *López and Okal,* 2006]. This inherent slowness may be detected by making simple, yet robust and rapid measurements targeting widely different properties of the seismic source. One such approach is the computation of radiated seismic energy, obtained by integrating the squared ground velocity as

recorded in teleseismic generalized-*P* wavetrains. Following the method of *Boatwright and Choy* [1986], *Newman and Okal* [1998] have developed an algorithm providing an estimate E^E of the radiated energy, while ignoring source details unavailable in real time, such as exact focal mechanism and source depth. They then compare it with the seismic moment M_0 of the source, through a "slowness" parameter

$$\Theta = \log_{10} \frac{E^E}{M_0} \tag{9}$$

Scaling laws would predict a constant value of –4.90 for Θ, which is indeed close to the worldwide average computed on a population of regular earthquakes. On the other hand, and as shown on Fig. 5-11, "tsunami earthquakes" feature significantly depleted values of Θ, deficient by typically 1 to 2 units, the use of a logarithmic scale giving particular robustness to the concept. The algorithm has been implemented as part of the real-time assessment of teleseismic events at the Pacific Tsunami Warning Center [*Weinstein and Okal,* 2005]. Incidentally, higher-than-normal values of Θ are characteristic of "snappy" earthquakes, featuring greater stress drops, and hence higher accelerations and producing more damage than

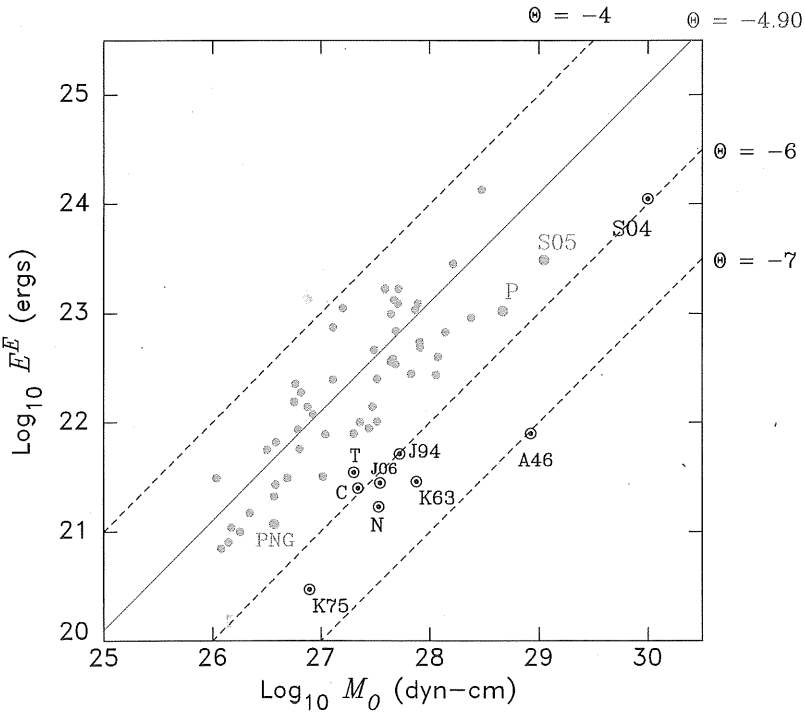

Fig. 5.11 – Logarithmic plot of Estimated Energy E^E computed for 54 recent earthquakes, *vs.* Harvard CMT seismic moment M_0. Dashed lines are drawn for constant Θ with the value predicted by scaling laws (–4.90) shown solid. Dark bull's eye symbols identify "tsunami earthquakes", listed in Table 2. Other events shown include Peru 2001 (P), Papua New Guinea 1998 (PNG) and Nias-Simeulue 2005 (S05). Updated from *Newman and Okal* [1999].

expected from seismic moments. Examples include such intraplate earthquakes as the 1939 Chillan, Chile and 1999 Oaxaca, Mexico earthquakes [*Okal and Kirby,* 2002], and the recent Central Kuriles earthquake of 13 January 2007. Finally, note that the concept of Θ shares its philosophy of comparing two measurements made at different periods with the time-honored $m_b : M_s$ discriminant, introduced to identify large explosions [*e.g., Marshall and Basham,* 1972].

Along similar lines, *Okal et al.* [2003] have documented that "tsunami earthquakes" are also noticeably deficient in the generation of hydroacoustic *T* phases, and quantified this property through a parameter Γ expressing the ratio of *T*–phase energy flux to seismic moment. They show deficiencies of as much as two orders of magnitude for "tsunami earthquakes", as well as an excellent correlation between Γ and Θ [*Okal,* 2007*b*]. However, because *T* phases travel slower than seismic waves, they bear less promise towards real-time tsunami warning.

Finally, following a remark by *Ni et al.* [2005], *Reymond and Okal* [2006] have shown that source duration can be meaningfully extracted from the generalized *P* wave of teleseismic records by band-pass filtering in the 2–4 Hz high-frequency range, thus eliminating later phases whose contributions may affect the more conventional properties of *P* waves for long source durations. These authors concluded that this procedure recovers the exceptional duration of mega earthquakes such as the 2004 Sumatra-Andaman event, and of some (but unfortunately not all) "tsunami earthquakes". Thus, while this approach holds promise for the early detection of "tsunami earthquakes", more research is clearly needed in this area.

Any progress regarding the mitigation of the risk from "tsunami earthquakes" will obviously require an understanding of the conditions leading to their exceptional source slowness, and of whether such behavior can be realistically predicted in recognizable tectonic environments. In this framework, *Okal and Newman* [2001] conducted a detailed analysis of the parameter Θ in the three subduction zones where "tsunami earthquakes" occurred during the 1990s (Central America, Java and Northern Peru), and concluded that regional background seismicity at lower magnitudes did not share anomalously low values of Θ, which suggests that slowness, at least in those subduction zones, would require a minimum size of earthquake, in turn hinting at source complexity as a potential requirement for slow earthquakes. In addition, they confirmed the 1960 event in Northern Peru, about 350 km NW of Chimbote, as a "tsunami earthquake", with a parameter Θ comparable to that of the 1996 event. This suggests that common conditions along a subduction zone may give it a uniform potential for "tsunami earthquakes". Posterior to their study, the recent occurrence of the 2006 "tsunami earthquake" in Java [*Reymond and Okal,* 2006], 600 km to the West of the 1994 epicenter, lends considerable support to this suggestion. Finally, *Okal and Newman* [2001] noted that no very large interplate thrust earthquakes ($M_0 \geq 3 \times 10^{28}$ dyn*cm) were documented in the instrumental (and available historical) seismic record of any of the three relevant subduction zones, leading to the legitimate question of whether the occurrence of "tsunami earthquakes" can exclude that of mega-thrust earthquakes in the same region. In the framework of our newly revised concepts regarding the maximum size of earthquakes at subduction zones [*Stein and Okal,* 2007], and given that the 1946 Aleutian "tsunami earthquake" is itself very large [*López and Okal,* 2006], this question must be considered wide open, but is of course of con-

siderable interest, for example regarding tsunami risk in Australia from earthquakes in the Java trench.

Regarding the nature of potential tectonic environments for the generation of "tsunami earthquakes", two classes of models have been proposed. The first one consists of events rupturing through shallow material featuring poor mechanical properties, such as accretionary prisms, as exemplified by the 1896 Sanriku event [*Tanioka and Satake,* 1996*b*], and the 1963 (20 October) and 1975 Kuriles earthquakes [*Fukao,* 1979]. Note that the latter two can be regarded as aftershocks, occurring on nearby splay faults, of larger shocks with conventional rupture properties, namely the great 1963 (13 October) Kuriles earthquake and the 1973 Nemuro-Oki event. The lesser rigidity of the source region of the "tsunami earthquake" would explain the greater excitation of tsunami waves, following the results of *Okal* [1988] discussed above, as well as the reduced rupture velocity V_R leading to exceptional source slowness and destructive interference for higher-frequency waves. The probable "tsunami earthquakes" of 13 April 1923 in Kamchatka (following the great interplate thrust earthquake of 03 February 1923) and 22 June 1932 in Mexico (following the Colima event of 03 June 1932) may also fit this pattern.

By contrast, a second class of models for "tsunami earthquakes" considers a sediment-starved environment leading to a partially decoupled interface between the downgoing slab and the overriding plate [*Tanioka et al.,* 1997]. The absence of a sedimentary plug may allow the upward propagation of rupture rather than the creep generally prevailing along the shallowest portion of the interface [*Byrne et al.,* 1988]. In the presence of irregular bathymetry on the subducting ocean floor, the interface is expected to be jagged and the upward rupture will be irregular and, on the average, slow. This model was expanded by *Polet and Kanamori* [2000] and applied to the 1992 Nicaragua, 1994 Java and 1996 Chimbote, Peru "tsunami earthquakes". It does hold a promise for interpreting this class of "tsunami earthquakes" in a tectonic context, giving them some level of geographic predictability.

We include the 2004 Sumatra-Andaman earthquake in the list of "tsunami earthquakes" in Table 2, based on several lines of evidence. It has generally been very difficult to obtain the source parameters of this event, as routine measuring algorithms were simply not adapted to its exceptional size; examples would include the target frequency of moment tensor inversions from surface waves, or at the other end of the spectrum, the duration of integration windows of generalized P waves for the computation of radiated energy. As a result, there remains some uncertainty, and even controversy, regarding the final values of moment M_0 and energy E^E. We use here the moment of 1.1×10^{30} dyn*cm derived by *Stein and Okal* [2005] from the analysis of the Earth's gravest modes, in excellent agreement with the composite moment tensor inversion of *Tsai et al.* [2005] (1.16×10^{30} dyn*cm), and the radiated energy estimated at 1.4×10^{24} ergs by *Choy and Boatwright* [2007], who used a special algorithm eliminating the influence of later phases. This translates into a slowness parameter $\Theta = -5.89$, roughly one unit less than predicted by scaling laws, and essentially equivalent to that of the 1996 Chimbote, Peru earthquake, thus qualifying the 2004 Sumatra-Andaman earthquake as a "tsunami earthquake". In addition, detailed studies in source tomography based on traditional seismic waves [*Ishii et al.,* 2005], the generation of T phases [*de-Groot-Hedlin,* 2005; *Tolstoy and Bohnenstiehl,* 2005; *Guilbert et al.,* 2005] or the

composite inversion by *Tsai et al.* [2005] all lead to an average rupture velocity of 2.7 km/s, which is significantly less than the value of 3.5 km/s predicted under scaling laws. Furthermore, all these models suggest a slowing down of the rupture towards the North, to values of ~ 2.0 km/s or less, also in agreement with the conclusions of *Choy and Boatwright* [2007], further suggesting that the 2004 earthquake may have featured increasing slowness in the later part of its rupture, as also discussed by *Seno and Hirata* [2007]. Finally, from a qualitative standpoint, it is interesting to note that many pictures and videos of the inundation of Banda Aceh by the tsunami show that most buildings were standing unaffected by the earthquake before they were taken down by the tsunami, confirming a deficiency of high-frequency components in the source. While not reaching the record values of slowness of the 1946 Aleutian earthquake, or even the 1992 Nicaragua event, the 2004 Sumatra shock clearly features a source spectrum which cannot be explained by simply extrapolating universal scaling laws to its exceptional size.

We wish to stress, however, that the qualification of the 2004 Sumatra event as a "tsunami earthquake" may be controversial, depending on the particular definition of such events. We note in particular that a definition such as *"an event whose tsunami has significantly larger amplitude than expected from estimates of its size obtained from seismic waves"*, will depend on the particular nature of such estimates. Earthquakes whose source violates scaling laws will feature moment estimates crucially dependent on the period of the measurement; in their aftermath, scientists will make increasingly sophisticated measurements, in practice at increasingly long periods. Eventually, the seismic models obtained will provide adequate representations of the source of the tsunami. This was the case, for example, with the 1946 Aleutian earthquake: its moment estimates using 100–s waves [*Brune and Engen,* 1969; *Kanamori,* 1972] or *a fortiori* 20–s M_s measurements [*Gutenberg and Richter,* 1954] led to deficiencies in tsunami excitation, but the far-field tsunami could be successfully modeled from *López and Okal*'s [2006] very-low frequency seismic model, obtained at 250 s [*Okal and Hébert,* 2007]. The situation was remarkably similar in the case of the Sumatra event: early estimates of its seismic moment (*e.g.,* original Harvard CMT solution using 300–s waves) are clearly incompatible with observed run-up values under the Plafker rule of thumb, while the tsunami can be successfully modeled using the more definitive moment values obtained later by investigators working at much longer periods [*Stein and Okal,* 2005; *Tsai et al.,* 2005]. Indeed, one could make the provocative statement that the characterization of an event as a "tsunami earthquake" under the above definition is transient in time, and that given enough time, seismologists will come up with a model explaining the generation of both seismic and tsunami waves. A better definition of a "tsunami earthquake" should focus on the disparity of its properties in terms of its tsunami and its [most conventional] seismic waves, which expresses a violation of the paradigm commonly used to relate them, in other words of seismic scaling laws. It is in this respect that the 2004 Sumatra earthquake can qualify as a "tsunami earthquake".

Among mega-thrust earthquakes, the 1960 Chilean event (total moment $M_0 = 5 \times 10^{30}$ dyn*cm) was also determined to have involved an ultra-slow component to its source, in that case as a precursor [*Kanamori and Cipar,* 1974; *Kanamori and Anderson,* 1975; *Cifuentes and Silver,* 1989], although the absence of adequate digital records makes it impossible to formally compute a parameter Θ. On the

other hand, the 2005 Nias-Simeulue earthquake features no more than a trend towards slowness ($\Theta = -5.54$), common to many other earthquakes in subduction zones. Thus excessive source slowness may not be a necessary feature of all megathrust events.

Finally, we want to stress that we do not categorize as genuine "tsunami earthquakes" those events for which exceptionally large local tsunamis resulted from a phenomenon ancillary to the seismic rupture, namely the triggering of an underwater landslide, the most dramatic example being the Papua New Guinea event of 17 July 1998 [*Synolakis et al.,* 2002]. In particular, we reemphasize that all large earthquakes can trigger landslide failures in precarious materials, which in turn can generate tsunamis with run-up values locally much larger than those of the parent earthquake. For example, during the Flores, Indonesia earthquake of 02 December 1992, which featured no clear anomaly in its seismic source properties, run-up reached a catastrophic 26 m at Riang-Kroko Village, as opposed to an average of 4–5 m at other locations along the Northern Coast of Flores Island [*Tsuji et al.,* 1995*b*]. Underwater surveys [*Plafker,* 1997] later identified submarine landslides triggered locally by the earthquake, as the probable source of such inconsistent run-up values. This interpretation is also likely for the exceptional run-up of 21 m observed at Nusa Kambangan during the 2006 Java tsunami [*Fritz et al.,* 2006*a*].

7. Conclusion

In conclusion, this Chapter has reviewed the theoretical bases of our present understanding of the excitation of tsunamis by earthquake sources. The exceptional character of tsunamis as natural hazards results from their ability to export death and destruction across the largest oceanic basins. In this respect, a very large seismic moment is clearly a pre-requisite for fatalities in the far field. However, the dataset in Table 1 clearly shows that other factors can affect the impact of a transoceanic tsunami. Among them, directivity is the most important one, explaining the patterns of loss of life in the far field in 1946, 1960, 1964 and 2004. By contrast, the 1963 Kuriles and 1965 Rat Island earthquakes had directivity lobes at azimuths N133°E and 200°E, respectively 33° and 61°E away from the direction of Hawaii. There are no high (volcanic) islands lying in the lobes of directivity for their tsunamis, only the sparsely populated atolls of Micronesia and the Marshall Islands. Such structures featuring small islands with steep underwater slopes, disfavor shoaling and run-up by long waves, as observed in the Maldives during the 2004 Sumatra-Andaman tsunami [*Fritz et al.,* 2006*b*]. This explains the lack of damage and fatalities from the tsunamis of 1963 and 1965 in the far field.

The case of the 1952 Kamchatka and 1957 Aleutian Islands events is more puzzling. These were truly huge earthquakes, even though some uncertainty remains regarding the seismic moment of the latter [*Johnson et al.,* 1994]. Documents released during the 1990s indicate that the 1952 tsunami totally destroyed the city of Severo-Kuril'sk and the adjacent Soviet Navy base, with a death toll estimated as high as 14,000 [*Kaistrenko and Sedaeva,* 2001]. As expected from its directivity lobe oriented N122°E, only 5° away from the azimuth of Hawaii, the tsunami impacted the Hawaiian Islands, resulting in considerable flooding and damage, as did the 1957 Aleutian earthquake, whose directivity lobe is within a few degrees of the azimuth to Hawaii. Miraculously, neither of the two events caused any deaths in

Hawaii; by contrast, 61 lives were lost in Hawaii during the 1960 Chilean tsunami. *Fraser et al.*'s [1959] account of the 1957 event reports what amounts to a conservatively cautious warning which, most importantly, was well heeded by the population, whereas the 1960 warning was poorly understood by the residents, and actually called off by officials after the first wavetrains [*Eaton et al.,* 1961].

As for the 2005 Nias event, in addition to the small far field tsunami reflecting the shallow bathymetry and presence of islands at the source, the absence of tsunami casualties in the near field can be attributed to the combination of a population educated by oral tradition, a strong coseismic uplift on Simeulue Island which helped reduce the impact of the wave, and the fact that many residents were living in refugee camps inland as a result of the December 2004 event [*McAdoo et al.,* 2006].

As detailed in this chapter, we now understand many facets of tsunami generation by earthquakes. Yet, as Table 1 shows, even the largest events can generate tsunamis of widely varying impact, both in the far field and, perhaps more surprisingly, in the near field as well. After fifty years, *Fraser et al.*'s [1959] remark quoted in the epigraph and written in the wake of the 1957 Aleutian tsunami, still prevails. Only through more research on past and future tsunamis, and through the education of populations at risk, will tragedies comparable to the 2004 Sumatra-Andaman tsunami be avoided in the future.

Appendix

We compute the energy transferred to the tsunami in the framework of Fig. 5-02. Assuming that a hump is created on the sea surface above the deformed section of the ocean bottom, the work W necessary to lift a mass $\rho_w S\, \delta h$ of water over the height H of the ocean column is

$$W = \rho_w S\, \delta h \cdot g \cdot H \tag{A1}$$

which is also the work of the pressure forces at the sea bottom, $\rho_w gH \cdot S$, displacing the ocean floor an amount δh. This work will be applied in part towards changing the potential energy E_p of the relevant mass of water between its average heights above undeformed sea floor, $\delta h/2$ in the original state *(a)* and H in the final state

$$\Delta E_p = \rho_w S\, \delta h \cdot g \cdot \left(H - \frac{\delta h}{2} \right) \tag{A2}$$

The difference $W - \Delta E_p$ is the energy of the tsunami:

$$E_T = \frac{1}{2} \rho_w g\, S\, (\delta h)^2 \tag{A3}$$

It can also be interpreted as the release of the potential energy of the unstable hump *(b)* as it collapses on the ocean surface *(e)*. Note in particular that this energy, growing like $(\delta h)^2$ is always positive, regardless of the sign of δh.

If the deformation were to proceed slowly and reversibly, without the creation of the hump, the pressure at the bottom would vary over the course of the deformation, adjusting from $\rho_w g H$ to $\rho_w g (H - \delta h)$, leading to W exactly equal to ΔE_p, as given by (A2), with no energy available to generate a tsunami.

Under earthquake scaling laws, all linear dimensions in (A3) are expected to grow like seismic slip Δu or equivalently fault length L, leading to E_T proportional to L^4, or $M_0^{4/3}$. This dependence was formally derived by *Kajiura* [1981], who proposed the expression

$$(E_T)_{Kaj.} = \frac{F_{Kaj.}}{2^{4/3}} \cdot \frac{\rho_w g}{\mu^{4/3}} \varepsilon_{\max}^{2/3} \cdot M_0^{4/3} \tag{A4}$$

where $F_{Kaj.}$ is the square of the dimensionless ratio of δh to the slip Δu, averaged over focal geometries and hypocentral depths. *Okal* [2003] has derived a very similar expression

$$(E_T)_{modes} = 0.22 \cdot \frac{\rho_w g}{\mu^{4/3}} \varepsilon_{\max}^{2/3} \cdot M_0^{4/3} \tag{A5}$$

by integrating over frequency the power spectrum density of the individual tsunami modes, weighted by their expected excitation and taking into account the source spectrum and its seismic corner frequencies. Note that (A3), (A4) and (A5) do not depend on the depth H of the oceanic column.

Acknowledgments

I am indebted to Costas Synolakis for many years of friendship and collaboration. A special word of appreciation goes to George Plafker for instilling in my mind the concept of the "Plafker rule of thumb" while roaming the fog-shrouded, bear-infested beaches of Unimak Island in 2001. I also thank many other scientists, too numerous to list individually, for enlightening my vision of tsunamis. The preparation of this chapter was supported by the National Science Foundation, under Grant CMS-03-01054.

References

Abe, Ka., A new scale of tsunami magnitude, M_t, **in:** *Tsunamis — their science and engineering,* ed. by K. Iida and T. Iwasaki, pp. 91–101, TERRA- PUB, Tokyo, 1983.

Abe, Ka., Quantification of tsunamigenic earthquakes by the M_t scale, *Tectonophysics,* **166,** 27-34, 1989.

Abe, Ku., A dislocation model of the 1933 Sanriku earthquake consistent with the tsunami waves, *J. Phys. Earth,* **26,** 381–396, 1978.

Abe, Ku., Ka. Abe, Y. Tsuji, F. Imamura, H. Katao, I. Yohihisa, K. Satake, J. Bourgeois, E. Noguera, and F. Estrada, Field survey of the Nicaragua earthquake and tsunami of September 2, 1992, *Bull. Earthq. Res. Inst. Tokyo Univ.,* **68,** 23–70, 1993.

Aki, K., Generation and propagation of *G*-waves from the Niigata earthquake of June 16, 1964. Part 2. Estimation of earthquake moment, released energy, and stress-strain drop from the *G*-wave spectrum, *Bull. Earthq. Res. Inst. Tokyo Univ.,* **44,** 73–88, 1966.

Aki, K., and P. G. Richards, *Quantitative Seismology,* W. H. Freeman, San Francisco, 932 pp., 1980.

Artru, J., V. Dučić, H. Kanamori, P. Lognonné, and M. Murakami, Ionospheric detection of gravity waves induced by tsunamis, *Geophys. J. Intl.,* **160,** 840–848, 2005.

Banerjee, P., F. Pollitz, B. Nagarajan, and R. Bürgmann, Coseismic slip distributions of the 26 December 2004 Sumatra-Andaman and 28 March 2005 Nias earthquakes from GPS static offsets, *Bull. Seismol. Soc. Amer.,* **87,** S86–S102, 2007.

Ben-Menahem, A., Radiation of seismic surface waves from finite moving sources, *Bull. Seismol. Soc. Amer.,* **51,** 401–435, 1961.

Ben-Menahem, A., and M. Rosenman, Amplitude patterns of tsunami waves from submarine earthquakes, *J. Geophys. Res.,* **77,** 3097–3128, 1972.

Boatwright, J., and G. L. Choy, Teleseismic estimates of the energy radiated by shallow earthquakes , *J. Geophys. Res.,* **91,** 2095–2112, 1986.

Borrero, J. C., Field data and satellite imagery of tsunami effects in Banda Aceh, *Science,* **308,** 1596, 2005.

Borrero, J. C., M. Ortiz, V. V. Titov, and C. E. Synolakis, Field survey of Mexican tsunami produced new data, unusual photos, *Eos, Trans. Amer. Geophys. Un.,* **78,** 85 and 87–88, 1997.

Borrero, J. C., R Hidayat, Suranto, C. Bosserelle, and E. A. Okal, Field survey and preliminary modeling of the near-field tsunami from the Bengkulu earthquake of 12 September 2007, *Eos, Trans. Amer. Geophys. Un.,* **88,** *(52),* U54A-04, 2007 [abstract].

Bourgeois, J., C. Petroff, H. Yeh, V. V. Titov, C. E. Synolakis, B. Benson, J. Kuroiwa, J. Lander, and E. Norabuena, Geologic setting, field survey and modeling of the Chimbote, northern Peru tsunami of 21 February 1996, *Pure Appl. Geophys.,* **154,** 513–540, 1999.

Bourgeois, J., T. Pinegina, N. Razhegaeva, V. Kaistrenko, B. Levin, B. MacInnes, and E. Kravchunovskaya, Tsunami runup in the Middle Kuril Islands from the great earthquake of 15 November 2006, *Eos, Trans. Amer. Geophys. Un.,* **88,** *(52),* S51C-02, 2007 [abstract].

Brune, J. N., and G. R. Engen, Excitation of mantle Love waves and definition of mantle wave magnitude, *Bull. Seismol. Soc. Amer.,* **59,** 923–933, 1969.

Byrne, D. E., D. M. Davis, and L. R. Sykes, Loci and maximum size of thrust earthquakes and the mechanisms of the shallow region of subduction zones, *Tectonics,* **7,** 833–857, 1988.

Choy, G. L., and J. Boatwright, The energy radiated by the 26 December 2004 Sumatra-Andaman earthquake estimated from 10-minute *P*-wave windows, *Bull. Seismol. Soc. Amer.,* **97,** S18–S24, 2007.

Cifuentes, I. L., and P. G. Silver, Low-frequency source characteristics of the great 1960 Chilean earthquake, *J. Geophys. Res.,* **94,** 643–663, 1989.

Dahlen, F. A., Single force representation of shallow landslide sources, *Bull. Seismol. Soc. Amer.,* **83,** 130–143, 1993.

de Groot-Hedlin C. D., Estimation of the rupture length and velocity of the great Sumatra earthquake of Dec. 26, 2004 using hydroacoustic signals, *Geophys. Res. Letts.,* **32,** *(11),* L11303, 4 pp., 2005.

Dziewonski, A. M., A.-T. Chou, and J. H. Woodhouse, Determination of earthquake source parameters from waveform data for studies of global and regional seismicity, *J. Geophys. Res.,* **86,** 2825–2852, 1981.

Eaton, J. P., D. H. Richter, and W. U. Ault, The tsunami of May 23, 1960 on the Island of Hawaii, *Bull. Seismol. Soc. Amer.,* **51,** 135–157, 1961.

Farreras, S. F., and A. J. Sanchez, The tsunami threat on the Mexican West coast: A historical analysis and recommendations for hazard mitigation, *Natur. Haz.,* **4,** 301–316, 1991.

Fraser, G. D., J. P. Eaton, and C. K. Wentworth, The tsunami of March 9, 1957 on the Island of Hawaii, *Bull. Seismol. Soc. Amer.,* **49,** 79–90, 1959.

Fritz, H. M., and J. C. Borrero, Somalia field survey after the December 2004 Indian Ocean tsunami, *Earthquake Spectra,* **22,** S219–S233, 2006.

Fritz, H., J. Goff, C. Harbitz, B. McAdoo, A. Moore, H. Latief, N. Kalligeris, W. Kodjo, B. Uslu, V. Titov, and C. Synolakis, Survey of the July 17, 2006 Central Java tsunami reveals 21 m runup heights, *Eos, Trans. Amer. Geophys. Un.,* **87,** *(52),* S14A-06, 2006*a* [abstract].

Fritz, H. M., C. E. Synolakis, and B. G. McAdoo, Maldives field survey after the December 2004 Indian Ocean tsunami, *Earthquake Spectra,* **22,** S137-S154, 2006*b*.

Fukao, Y., Tsunami earthquakes and subduction processes near deep-sea trenches, *J. Geophys. Res.,* **84,** 2303–2314, 1979.

Geller, R. J., Scaling relations for earthquake source parameters and magnitudes, *Bull. Seismol. Soc. Amer.,* **66,** 1501–1523, 1976.

Gilbert, F., Excitation of the normal modes of the Earth by earthquake sources, *Geophys. J. Roy. astron. Soc.,* **22,** 223–226, 1970.

Gilbert, F, and A. M. Dziewonski, An application of normal mode theory to the retrieval of structural parameters and source mechanisms from seismic spectra, *Phil. Trans. Roy. Soc. London, Ser. A,* **278,** 187–269, 1975.

Goffe, J., P. L.-F. Liu, B. Higman, R. Morton, B. E. Jaffe, H. Fernando, P. Lynett, H. Fritz, C. Synolakis, and S. Fernando, Sri Lanka field survey after the December 2004 Indian Ocean tsunami, *Earthquake Spectra,* **22,** S173–S186, 2006.

González, F. I., C. L. Mader, M. Eble, and E. N. Bernard, The 1987–88 Alaskan Bight Tsunamis: Deep ocean data and model comparisons, *Nat. Hazards,* **4,** 119–139, 1991.

González, F. I., E. N. Bernard, C. Meinig, M. C. Eble, H. O. Mofjeld, and S. Stalin, The NTHMP tsunameter network, *Nat. Hazards,* **35,** 25–39, 2005.

Guilbert, J., J. Vergoz, E. Schisselé, A. Roueff, and Y. Cansi, Use of hydroacoustic and seismic arrays to observe rupture propagation and source extent of the M_w = 9.0 Sumatra earthquake, *Geophys. Res. Letts.,* **32,** *(15),* L15310, 5 pp., 2005.

Gutenberg, B., and C. F. Richter, Seismicity of the Earth, *Geol. Soc. Amer. Spec. Pap.,* **34,** 125 pp., 1941.

Gutenberg, B., and C. F. Richter, *Seismicity of the Earth and associated phenomena,* Princeton Univ. Press, Princeton, N.J., 308 pp., 1954.

Harkrider, D. G., C. A. Newton, and E. A. Flinn, Theoretical effect of yield and burst height of atmospheric explosions on Rayleigh wave amplitudes, *Geophys. J. Roy. astr. Soc.,* **36,** 191–225, 1974.

Haskell, N. A., A note on air-coupled surface waves, *Bull. Seismol. Soc. Amer.,* **41,** 295–300, 1951.

Hwang, L.-S., H. L. Butler, and D. J. Divoky, Tsunami mode: generation and open sea characteristics, *Bull. Seismol. Soc. Amer.,* **62,** 1579–1596, 1972.

Imamura, F., C. E. Synolakis, E. Gica, V. Titov, E. Listanco, and H. J. Lee, Field survey of the 1994 Mindoro Island, Philippines, tsunami, *Pure Appl. Geophys.,* **144,** 875–890, 1995.

Ishii, M., P. Shearer, H. Houston, and J. E. Vidale, Extent, duration and speed of the 2004 Sumatra-Andaman earthquake imaged by Hi-Net array, *Nature,* **435,** 933–936, 2005.

Iwasaki, S. I., Experimental study of a tsunami generated by a horizontal motion of a sloping bottom, *Bull. Earthq. Res. Inst. Tokyo Univ.,* **57,** 239–262, 1982.

Johnson, J. M., Y. Tanioka, L. J. Ruff, K. Satake, H. Kanamori, and L. R. Sykes, The 1957 great Aleutian earthquake, *Pure Appl. Geophys.,* **142,** 3–28, 1994.

Kaistrenko, V. M., and V. M. Sedaeva, 1952 North Kuril tsunami: new data from archives, **in:** *Tsunami research at the end of a critical decade,* ed. by G. T. Hebenstreit, pp. 91–102, Kluwer, Netherlands, 2001.

Kajiura, K., Tsunami energy in relation to parameters of the earthquake fault model, *Bull. Earthq. Res. Inst. Tokyo Univ.,* **56,** 415–440, 1981.

Kanamori, H., Synthesis of long-period surface waves and its application to earthquake source studies—Kurile Islands earthquake of October 13, 1963, *J. Geophys. Res.,* **75,** 5011–5027, 1970*a*.

Kanamori, H., The Alaska earthquake of 1964: Radiation of long-period surface waves and source mechanism, *J. Geophys. Res.,* **75,** 5029–5040, 1970*b*.

Kanamori, H., Seismological evidence for a lithospheric normal faulting—The Sanriku earthquake of 1933, *Phys. Earth Planet. Inter.,* **4,** 289–300, 1971.

Kanamori, H., Mechanism of tsunami earthquakes, *Phys. Earth Planet. Inter.,* **6,** 346–359, 1972.

Kanamori, H., The energy release in great earthquakes, *J. Geophys. Res.,* **82,** 2981–2987, 1977.

Kanamori, H., and D. L. Anderson, Theoretical basis of some empirical relations in seismology, *Bull. Seismol. Soc. Amer.,* **65,** 1073–1095, 1975.

Kanamori, H., and J. J. Cipar, Focal processes of the Great Chilean earthquake May 22, 1960, *Phys. Earth Planet. Inter.,* **9,** 128–136, 1974.

Kato, K., and Y. Tsuji, Tsunami of the Sumbawa earthquake of August 19, 1977, *J. Natur. Disaster Sci.,* **17,** 87–100, 1995.

Kerr, R. A., Model shows islands muted tsunami after latest Indonesian quake, *Science,* **308,** 341, 2005.

Knopoff, L., and F. Gilbert, Radiation from a strike-slip earthquake, *Bull. Seismol. Soc. Amer.,* **49,** 163–178, 1959.

Kulikov, E. A., P. P. Medvedev, and S. S. Lappo. Satellite recording of the Indian Ocean tsunami on December 26, 2004, *Doklady Earth Sci.,* **401,** 444–448, 2005.

López, A. M., and E. A. Okal, A seismological reassessment of the source of the 1946 Aleutian "tsunami" earthquake, *Geophys. J. Intl.,* **165,** 835–849, 2006.

Love, A. E. H., *Some problems in geodynamics,* Cambridge Univ. Press, 1911.

Lundgren, P. R., and E. A. Okal, Slab decoupling in the Tonga arc: the June 22, 1977 earthquake, *J. Geophys. Res.,* **93,** 13355–13366, 1988.

Macdonald, G. A., and C. K. Wentworth, The tsunami of November 4, 1952 on the Island of Hawaii, *Bull. Seismol. Soc. Amer.,* **44,** 463–469, 1954.

Madariaga, R. I., Toroidal free oscillations of the laterally heterogeneous Earth, *Geophys. J. Roy. astr. Soc.,* **27,** 81–100, 1972.

Mansinha, L., and D. E. Smylie, The displacement fields of inclined faults, *Bull. Seismol. Soc. Amer.,* **61,** 1433–1440, 1971.

Marshall, P. D., and P. W. Basham, Discrimination between earthquakes and underground explosions using an improved M_s scale, *Geophys. J. Roy. astr. Soc.,* **28,** 431–458, 1972.

McAdoo, B. G., L. Dengler, G. Prasetya, and V. Titov, *Smong:* How an oral history saved thousands on Indonesia's Simeulue Island during the December 2004 and March 2005 tsunamis, *Earthquake Spectra,* **22,** S661–S669, 2006.

Menyaĭlov, A. A., Tsunami v Ust'-Kamchatskom raĭone, *Byull. Vulkan. Stantsii na Kamchat., Akad. Nauk SSSR,* **12,** 9–13, 1946 [in Russian].

Newman, A. V., and E. A. Okal, Teleseismic estimates of radiated seismic energy: The E/M_0 discriminant for tsunami earthquakes, *J. Geophys. Res.,* **103,** 26885–26898, 1998.

Ni, S., H. Kanamori, and D. V. Helmberger, D., High-frequency radiation from the 2004 Great Sumatra-Andaman earthquake *Nature,* **434,** 582, 2005.

Occhipinti, G., P. Lognonné, E. Alam Kherani, and H. Hébert, 3-Dimensional waveform modeling of ionospheric signature induced by the 2004 Sumatra tsunami, *Geophys. Res. Letts.,* **33,** *(20),* L20104, 5 pp., 2006.

Okada, Y., Surface deformation due to shear and tensile faults in a half-space, *Bull. Seismol. Soc. Amer.,* **75,** 1135–1154, 1985.

Okal, E. A., Mode-wave equivalence and other asymptotic problems in tsunami theory, *Phys. Earth Planet. Inter.,* **30,** 1–11, 1982.

Okal, E. A., Seismic parameters controlling far-field tsunami amplitudes: A review, *Natural Hazards,* **1,** 67–96, 1988.

Okal, E. A., Erratum [to "Seismic parameters controlling far-field tsunami amplitudes: A review"], *Natural Hazards,* **4,** 433, 1991.

Okal, E. A., Use of the mantle magnitude M_m for the reassessment of the seismic moment of historical earthquakes. I: Shallow events, *Pure Appl. Geophys.,* **139,** 17–57, 1992.

Okal, E. A., Normal modes energetics for far-field tsunamis generated by dislocations and landslides, *Pure Appl. Geophys.,* **160,** 2189–2221, 2003.

Okal, E. A., Seismic records of the 2004 Sumatra and other tsunamis: A quantitative study, *Pure Appl. Geophys.,* **164,** 325–353, 2007*a*.

Okal, E. A., The generation of *T* waves by earthquakes, *Adv. Geophys.,* **49,** 1–65, 2007*b*.

Okal, E. A., and H. Hébert, Far-field modeling of the 1946 Aleutian tsunami, *Geophys. J. Intl.,* **169,** 1229–1238, 2007.

Okal, E. A., and S. H. Kirby, Energy-to-moment ratios for damaging intraslab earthquakes: Preliminary results on a few case studies, *USGS Open File Rept.,* **02–328,** 127–131, 2002.

Okal, E. A., and D. R. MacAyeal, Seismic recording on drifting icebergs: Catching seismic waves, tsunamis and storms from Sumatra and elsewhere, *Seismol. Res. Letts.,* **77,** 659–671, 2006.

Okal, E. A., and A. V. Newman, Tsunami earthquakes: The quest for a regional signal, *Phys. Earth Planet. Inter.,* **124,** 45–70, 2001.

Okal, E. A., and B. A. Romanowicz, On the variation of *b*-value with earthquake size, *Phys. Earth Planet. Inter.,* **87,** 55–76, 1994.

Okal, E. A., and C. E. Synolakis, Theoretical comparison of tsunamis from dislocations and landslides, *Pure Appl. Geophys.,* **160,** 2177–2188, 2003.

Okal, E. A., and C. E. Synolakis, Source discriminants for near-field tsunamis, *Geophys. J. Intl.,* **158,** 899–912, 2004.

Okal, E. A., and J. Talandier, M_m: A variable period mantle magnitude, *J. Geophys. Res.,* **94,** 4169–4193, 1989.

Okal, E. A., and J. Talandier, Single-station estimates of the seismic moment of the 1960 Chilean and 1964 Alaskan earthquakes, using the mantle magnitude M_m, *Pure Appl. Geophys.,* **136,** 103–126, 1991.

Okal, E. A., and V. V. Titov: M_{TSU}: Recovering seismic moments from tsunameter records, *Pure Appl. Geophys.,* **164,** 355–378, 2007.

Okal, E. A., A. Piatanesi, and P. Heinrich, Tsunami detection by satellite altimetry, *J. Geophys. Res.,* **104,** 599–615, 1999.

Okal, E. A., C. E. Synolakis, G. J. Fryer, P. Heinrich, J. C. Borrero, C. Ruscher, D. Arcas, G. Guille, and D. Rousseau, A field survey of the 1946 Aleutian tsunami in the far field, *Seismol. Res. Letts.,* **73,** 490–503, 2002.

Okal, E. A., P.-J. Alasset, O. Hyvernaud, and F. Schindelé, The deficient *T* waves of tsunami earthquakes, *Geophys. J. Intl.,* **152,** 416–432, 2003.

Okal, E. A., A. Sladen, and E. A.-S. Okal, Rodrigues, Mauritius and Réunion Islands, field survey after the December 2004 Indian Ocean tsunami, *Earthquake Spectra,* **22,** S241–S261, 2006*a*.

Okal, E. A., H. M. Fritz, R. Raveloson, G. Joelson, P. Pančošková, and G. Rambolamanana, Madagascar field survey after the December 2004 Indian Ocean tsunami, *Earthquake Spectra,* **22,** S263–S283, 2006*b*.

Okal, E. ., J. Talandier, and D. Reymond, Quantification of hydrophone records of the 2004 Sumatra tsunami *Pure Appl. Geophys.,* **164,** 309–323, 2007.

Pančošková P., E. A. Okal, D. R. MacAyeal, and R. Raveloson, Delayed response of far-field harbors to the 2004 Sumatra tsunami: the role of high-frequency components, *Eos, Trans. Amer. Geophys. Un.,* **87,** *(52),* U53A-0021, 2006 [abstract].

Pekeris, C. L., and H. Jarosch, The free oscillations of the Earth, **in:** *Contributions in Geophysics in honor of Beno Gutenberg,* Edited by H. Benioff, M. Ewing, B. F. Howell, Jr., and F. Press, pp. 171–192, Pergamon, New York, 1958.

Peltier, W. R., and C. O. Hines, On the possible detection of tsunamis by a monitoring of the ionosphere, *J. Geophys. Res.,* **81,** 1995–2000, 1976.

Plafker, G. L., Catastrophic tsunami generated by submarine slides and backarc thrusting during the 1992 earthquake on Eastern Flores, Indonesia, *Geol. Soc. Amer. Abstr. with Prog.,* **29,** *(5),* 57, 1997 [abstract].

Plafker, G., and J. C. Savage, Mechanism of the Chilean earthquakes of May 21 and 22, 1960, *Geol. Soc. Amer. Bull.,* **81,** 1001–1030, 1970.

Polet, J., and H. Kanamori, Shallow subduction zone earthquakes and their tsunamigenic potential, *Geophys. J. Intl.,* **142,** 684–702, 2000.

Reymond, D., and E. A. Okal, Rapid, yet robust source estimates for challenging events: Tsunami earthquakes and mega-thrusts, *Eos, Trans. Amer. Geophys. Un.,* **87,** *(52),* S14A-02, 2006 [abstract].

Romanowicz, B. A., Strike-slip earthquakes on quasi-vertical transcurrent faults; inferences for general scaling relations, *Geophys. Res. Letts.,* **19,** 481–484, 1992.

Ruff, L. J., and H. Kanamori, Seismicity and the subduction process, *Phys. Earth Planet. Inter.,* **23,** 240–252, 1980.

Rundle, J. B., Derivation of the complete Gutenberg-Richter magnitude-frequency relation using the principle of scale invariance, *J. Geophys. Res.,* **94,** 12337–12342, 1989.

Saito, M., Excitation of free oscillations and surface waves by a point source in a vertically heterogeneous earth, *J. Geophys. Res.,* **72,** 3895–3904, 1967.

Satake, K., Effects of bathymetry on tsunami propagation: Application of ray tracing to tsunamis, *Pure Appl. Geophys.,* **126,** 28–35, 1988.

Scharroo, R., W. H. F. Smith, V. V. Titov, and D. Arcas, Observing the Indian Ocean tsunami with satellite altimetry, *Geophys. Res. Abs.,* **7,** 230, 2005 [abstract].

Schwarz, H.-U., *Subaqueous slope failures — Experiments and modern occurrences,* E. Schweizerbart'sche Verlagsbuchhandlung, 116 pp., Stuttgart, 1982.

Seno, T., and K. Hirata, Did the 2004 Sumatra-Andaman earthquake involve a component of tsunami earthquakes?, *Bull. Seismol. Soc. Amer.,* **97,** S296–S306, 2007.

Solov'ev, S. L., *Zemletryaseniya i tsunami 13 i 20 oktyabrya 1963 goda na Kuril'skikh ostrovakh,* Akad. Nauk SSSR, Sibirs. Otdel., 105 pp., Yuzhno- Sakhalinsk, 1965 [in Russian].

Solov'ev, S. L., and M. D. Ferchev, Summary of data on tsunamis in the USSR, *Bull. Council Seismol. Acad. Sci. USSR,* **9,** 23–55, transl. by W. G. Van Campen, Hawaii Inst. Geophys. Transl. Ser., 37 pp., Honolulu, 1961.

Solov'ev, S. L., and Ch. N. Go, Catalogue of tsunamis on the Western Shore of the Pacific Ocean, *Can. Transl. Fish. Aquat. Sci.,* **6077,** 437 pp., 1984.

Stein, S., and E. A. Okal, Size and speed of the Sumatra earthquake, *Nature,* **434,** 581–582, 2005.

Stein, S., and E. A. Okal, Ultra-long period seismic study of the December 2004 Indian Ocean earthquake and implications for regional tectonics and the subduction process, *Bull. Seismol. Soc. Amer.,* **97,** S279–S295, 2007.

Steketee, J. A., On Volterra's dislocations in a semi-infinite elastic medium, *Can. J. Phys.,* **36,** 192–205, 1958.

Synolakis, C. E., The runup of long waves, *Ph.D. Dissertation,* Calif. Inst. Technol., 228 pp., Pasadena, 1986.

Synolakis, C. E., and E. A. Okal, 1992–2002: Perspective on a decade of post-tsunami surveys, **in:** *Tsunamis: Case studies and recent developments,* ed. by K. Satake, *Adv. Natur. Technol. Hazards,* **23,** pp. 1–30, 2005.

Synolakis, C. E., and E. A. Okal, Far-field tsunami risk from mega-thrust earthquakes in the Indian Ocean, *Eos, Trans. Amer. Geophys. Un.,* **87,** *(52),* U53A-0040, 2006 [abstract].

Synolakis, C. E., J.-P. Bardet, J. C. Borrero, H. L. Davies, E. A. Okal, E. A. Silver, S. Sweet, and D. R. Tappin, The slump origin of the 1998 Papua New Guinea tsunami, *Proc. Roy. Soc. (London), Ser. A,* **458,** 763–789, 2002.

Synolakis, C. E., J. C. Borrero, H. M. Fritz, V. V. Titov, and E. A. Okal, Inundation during the 26 December 2004 tsunami, *Coastal Engineering 2006,* ed. by J. McKee Smith, pp. 1625–1637, Word Scientific, Singapore, 2007.

Tadepalli, S., and C. E. Synolakis, The runup of N – waves, *Proc. Roy. Soc. London, Ser. A,* **445,** 99–112, 1994.

Tadepalli, S., and C. E. Synolakis, Model for the leading waves of tsunamis, *Phys. Rev. Letts.,* **77,** 2141–2145, 1996.

Talandier, J., and E. A. Okal, Human perception of T waves: the June 22, 1977 Tonga earthquake felt on Tahiti, *Bull. Seismol. Soc. Amer.,* **69,** 1475–1486, 1979.

Talandier, J., and E. A. Okal, An algorithm for automated tsunami warning in French Polynesia, based on mantle magnitudes, *Bull. Seismol. Soc. Amer.,* **79,** 1177–1193, 1989.

Tang, L., M. C. Spillane, M. Eble, R. Weiss, V. V. Titov, and E. N. Bernard, The Tonga tsunami of May 3, 2006 : A comprehensive test for developing the NOAA tsunami forecast system, *Eos, Trans. Amer. Geophys. Un.,* **87,** *(52),* T-21F06, 2006 [abstract].

Tanioka, Y., and K. Satake, Tsunami generation by horizontal displacement of ocean bottom, *Geophys. Res. Letts.,* **23,** 861–864, 1996*a*.

Tanioka, Y., and K. Satake, Fault parameters of the 1896 Sanriku tsunami earthquake estimated from tsunami numerical modeling, *Geophys. Res. Letts.,* **23,** 1549–1552, 1996*b*.

Tanioka, Y., L. J. Ruff, and K. Satake, What controls the lateral variation of large earthquake occurrence along the Japan trench?, *Island Arc,* **6,** 261–266, 1997.

Tinti, S., and A. Armigliato, Single-force point-source static fields: an exact solution for two elastic half-spaces, *Geophys. J. Intl.,* **135,** 607–626, 1998.

Titov, V. V., and C. E. Synolakis, Numerical modeling of tidal wave run-up, *J. Waterw. Port Ocean Coastal Eng.,* **124,** 157–171, 1998.

Tolstoy, M., and D. R. Bohnenstiehl, Hydroacoustic constraints on the rupture duration, length and speed of the great Sumatra-Andaman earthquake, *Seismol. Res. Letts.,* **76,** 419–425, 2005.

Tsai, V. C., M. Nettles, G. Ekström, and A. M. Dziewonski, Multiple CMT analysis of the 2004 Sumatra earthquake, *Geophys. Res. Letts.,* **32,** *(17),* L17304, 4 pp., 2005.

Tsuji, Y., F. Imamura, H. Matsutomi, C. E. Synolakis, P. T. Nanang, Jumadi, S. Harada, S. S. Han, K. Arai, and B. Cook, Field survey of the East Java earthquake and tsunami of June 3, 1994, *Pure Appl. Geophys.,* **144,** 839–854, 1995*a*.

Tsuji, Y., H. Matsutomi, F. Imamura, M. Takeo, Y. Kawata, M. Matsuyama, T. Takahashi, Sunarjo, and P. Harjadi, Damage to coastal villages due to the 1992 Flores Island earthquake tsunami, *Pure Appl. Geophys.,* **144,** 481–524, 1995*b*.

Vvedenskaya, A. V., Opredelenie polej smeshchenii pri zemletryaseniyakh s pomoshchyu teorii dislokatsii, *Izv. Akad. Nauk SSSR, Ser. Geofiz.,* **6,** 277–284, 1956 [in Russian].

Ward, S. N., Relationship of tsunami generation and an earthquake source, *J. Phys. Earth,* **28,** 441–474, 1980.

Ward, S. N., On tsunami nucleation: I. A point source, *J. Geophys. Res.,* **86,** 7895–7900, 1981.

Ward, S. N., On tsunami nucleation: II. An instantaneous modulated line source, *Phys. Earth Planet. Inter.,* **27,** 273–285, 1982.

Weinstein, S. A., and E. A. Okal, The mantle wave magnitude M_m and the slowness parameter Θ: Five years of real-time use in the context of tsunami warning, *Bull. Seismol. Soc. Amer.,* **95,** 779–799, 2005.

Wells, D. L., and K. J. Coppersmith, New empirical relationships among magnitude, rupture length, rupture width, rupture area, and surface displacement, *Bull. Seismol. Soc. Amer.*, **84,** 974–1002, 1994.

Wiggins, R. A., A fast, new computational algorithm for free oscillations and surface waves, *Geophys. J. Roy. astr. Soc.*, **47,** 135–150, 1976.

Woodhouse, J. H., and F. A. Dahlen, The effect of a general aspherical perturbation on the free oscillations of the Earth, *Geophys. J. Roy. astr. Soc.*, **53,** 335–354, 1978.

Woods, M. T., and E. A. Okal, Effect of variable bathymetry on the amplitude of teleseismic tsunamis: a ray-tracing experiment, *Geophys. Res. Letts.*, **14,** 765–768, 1987.

Wu, F. T., and H. Kanamori, Source mechanism of the February 4, 1965 Rat Island earthquake, *J. Geophys. Res.*, **73,** 6082–6092, 1973.

Yuen, P. C., P. F. Weaver, R. K. Suzuki, and A. S. Furumoto, Continuous, traveling coupling between seismic waves and the ionosphere evident in May 1968 Japan earthquake data, *J. Geophys. Res.*, **74,** 2256–2264, 1969.

Zachariasen, J., K. Sieh, F. W. Taylor, R. L. Edwards, and W. S. Hantoro, Submergence and uplift associated with the giant 1833 Sumatran subduction earthquake; evidence from coral microatolls, *J. Geophys. Res.*, **104,** 895–919, 1999.